PHASE-DOMAIN SYNCHRONOUS GENERATOR MODEL FOR TRANSIENTS SIMULATION

by

KWOK-WAI LOUIE

B.Sc. (Physics), Simon Fraser University, 1989
B.A.Sc. (EE), The University of British Columbia, 1993

A THESIS SUBMITTED IN PARTIAL FULFILLMENT OF

THE REQUIREMENTS FOR THE DEGREE OF

MASTER OF APPLIED SCIENCE

in

THE FACULTY OF GRADUATE STUDIES

Department of Electrical Engineering

We accept this thesis as conforming to the required standard

THE UNIVERSITY OF BRITISH COLUMBIA

April 1995

In presenting this thesis in partial fulfilment of the requirements for an advanced degree at the University of British Columbia, I agree that the Library shall make it freely available for reference and study. I further agree that permission for extensive copying of this thesis for scholarly purposes may be granted by the head of my department or by his or her representatives. It is understood that copying or publication of this thesis for financial gain shall not be allowed without my written permission.

Department of Electrical Engineering

The University of British Columbia
Vancouver, Canada

Date April 26, 1995.

ABSTRACT

Three-phase synchronous generators which convert mechanical energy into electrical energy are the main power sources of power systems. In this thesis a phase-domain synchronous generator model which is developed directly in the stator reference frame is presented. The electrical and mechanical parts of a three-phase synchronous generator are separately modelled by two different sets of differential equations which are discretized with the trapezoidal rule of integration. These two parts are linked together by the rotor position angle and the electromagnetic torque generated by the interactions of the different magnetic fields, resulting in a linear generator model. In order to represent the generator more accurately, the linear generator model is modified to include magnetic saturation effects, resulting in a non-linear generator model. A formula is developed to account for the saturation as a function of the rotor angle and the total magnetomotive force angle. The machine parameters in the stator reference frame are obtained from the given characteristic quantities by a suitable data conversion scheme. To verify the linear generator model, a comparison between the simulation results of a three-phase short-circuit at the terminals of the machine obtained with the new linear model and the model in the EMTP is conducted.

TABLE OF CONTENTS

LIST OF TABLES

LIST OF FIGURES

ACKNOWLEDGEMENT

I would like to thank my wife **Sally Choo** for her constant support and encouragement. I send all my regards to **my parents** for their love and support.

I am indebted to my supervisor, **Dr. J. R. Marti**, for his constant guidance, constant encouragement, strong support, and indispensable role in the success of this thesis. I am very thankful to **Dr. H. W. Dommel** for his encouragement, useful suggestions in the project , and careful examination of this thesis. I express my gratitude to **Dr. L. M. Wedepohl** for his careful examination of this thesis.

I would also like to thank the fellow students in the power group of the Electrical Engineering Department at U.B.C. for providing a nice research environment.

Chapter One

INTRODUCTION

1.1 Motivation to Model Three-Phase Synchronous Generators

Three-phase synchronous generators are rotating machines which convert mechanical power into three-phase alternating electrical power. They form the principal sources of electrical energy in power systems. Thus the performance of the generators greatly influences the operation of the power network. To study the behaviour of the power system, the characteristics of the synchronous generators must be investigated very carefully.

There are different established methods in modelling a three-phase synchronous generator. However, most of these methods represent the generator in the rotor reference frame using Park's co-ordinate transformation to transfer the electrical quantities of the machine between the stator and the rotor reference frames. Although modelling a generator in the rotor reference frame makes the inductances of the magnetically coupled coils time invariant, the use of Park's co-ordinate transformation complicates the model. In order to more accurately and simply model a three-phase synchronous generator, the machine can be directly represented in the stator reference frame.

1.2 Work in this Thesis

In this thesis a three-phase synchronous generator model is intended to be developed directly in the stator reference frame. The derivation of the differential equations and the development of the discrete-time model of the machine are also presented. To facilitate the development of a computer-based simulator, the generator model is developed in the high-level computer language of Ada95. There are seven chapters in addition to this

introductory one in the thesis to describe the generator model in detail.

In Chapter Two, the physical description of the electrical part of a three-phase synchronous generator is given briefly. Then the differential equations of the machine's electrical part are derived directly in the stator reference frame. To represent the machine's electrical part more accurately, in Chapter Three corrections on the differential equations of the machine's electrical part are made. In order to complete the mathematical description of the generator, the differential equations of the machine's mechanical part are derived in the same reference frame in Chapter Four. Based on the differential equations of a three-phase synchronous generator, in Chapter Five the linear discrete-time model of the machine is developed in the stator reference frame with the trapezoidal integration rule. In the model development, the CDA method is applied in the computer algorithm[1,2]. In order to model the generator more closely, in Chapter Six the linear generator model is modified to include magnetic saturation effects in the machine. In modelling magnetic saturation effects in the generator, magnetizing curves of the machine are assumed to be the only available saturation data. To verify the generator model, in Chapter Seven the case of a three-phase short-circuit at the terminals of the generator is simulated by both the new model and the one in the EMTP. Finally, in Chapter Eight the conclusions of this thesis project are presented.

Chapter Two

MATHEMATICAL DESCRIPTION OF THE ELECTRICAL PART

2.1 Introduction

A three-phase synchronous generator essentially consists of a field structure and a set of armature coils. The armature windings usually operate at voltages that are considerably higher than that of the field winding and thus require more space for insulation. They are also subject to high transient currents and must have adequate mechanical strength. Therefore, in practice, the field winding is mounted on the rotor and the armature windings are placed on the stator[3]. The field winding carries direct current to produce a rotational magnetic field in the air gap between the stator and the rotor. In addition to the field winding there are two damper windings on the rotor: the D-damper winding and the Q-damper winding. The Magnetic axis of the D-damper winding coincides with the d-axis and the magnetic axis of the Q-damper winding is in parallel with the q-axis of the rotor. The damper windings are used to damp out the rotor's oscillations, to reduce overvoltages under certain short-circuit conditions, and to aid in synchronizing the machine. The three-phase windings of the armature are distributed in space 120° apart around the periphery of the inner face of the stator. These six coils are magnetically coupled. In steady state operation, when the rotor carrying the field winding's direct current is rotating at constant speed, a uniform rotating magnetic field is generated in the air gap between the rotor and the stator. Consequently, steady state voltages displaced by 120° in phase are produced in the armature windings, regardless of the speed of the rotational field. In this chapter, the differential equations of the generator's electrical part are derived.

2.2 Differential Equations of the Electrical Part

Figure 2.1 shows the cross section of a salient pole three-phase synchronous generator.

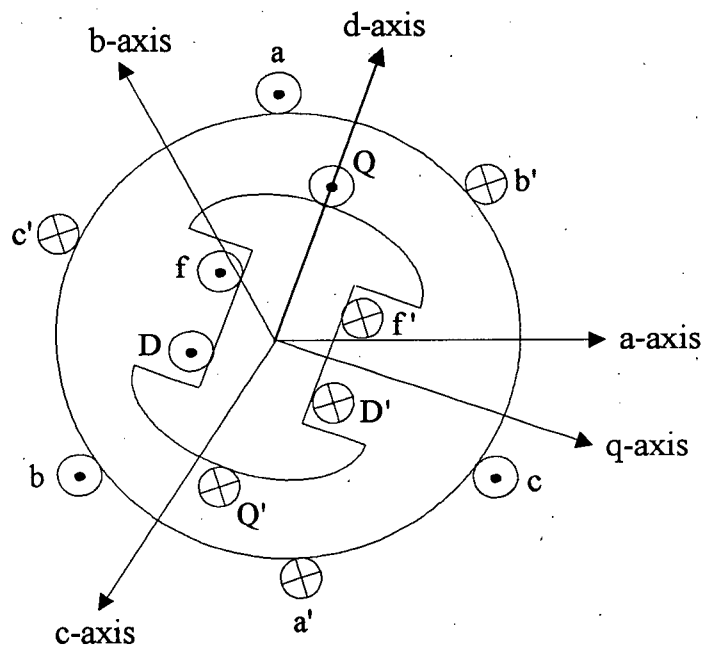

Figure 2.1 Cross Section of a Salient Pole Three-Phase Synchronous Generator

The electrical quantities of the generator can be represented mathematically. The derivation of the differential equations of the machine's electrical part are based on the following assumptions:

(1) The armature windings are distributed around the periphery of the inner face of the stator in such a manner that their self and mutual inductances are sinusoidal functions of the rotor position angle.

(2) The field structure windings are symmetrically placed about the d-axis and the q-axis on the rotor such that their self inductances and the mutual inductances are con

stant; however, the mutual inductance between a field structure winding and an armature winding is a sinusoidal function of the rotor position angle.

(3) The resistances of the six magnetically coupled windings are constant.

(4) The effects of the stator slots on the variation of any rotor inductance with rotor position angle are neglected;

(5) Saturation effects are not included (they are modelled in Chapter Six).

(6) The effects of hysteresis and eddy currents are neglected.

When the rotor is turning and its field winding is excited by a dc source, alternating voltages are induced in the armature windings. The voltage-current-flux relationships of the six magnetically coupled windings are given as follows:

$$[v(t)] = -[R][i(t)] - \frac{d}{dt}[\lambda(t)] \tag{2.1.1}$$

where

$$[v(t)] = \begin{bmatrix} v_a(t) \\ v_b(t) \\ v_c(t) \\ v_f(t) \\ 0 \\ 0 \end{bmatrix} \tag{2.1.2}$$

$$[R] = \begin{bmatrix} R_a & 0 & 0 & 0 & 0 & 0 \\ 0 & R_a & 0 & 0 & 0 & 0 \\ 0 & 0 & R_a & 0 & 0 & 0 \\ 0 & 0 & 0 & R_f & 0 & 0 \\ 0 & 0 & 0 & 0 & R_D & 0 \\ 0 & 0 & 0 & 0 & 0 & R_Q \end{bmatrix} \tag{2.1.3}$$

$$[i(t)] = \begin{bmatrix} i_a(t) \\ i_b(t) \\ i_c(t) \\ i_f(t) \\ i_D(t) \\ i_Q(t) \end{bmatrix} \tag{2.1.4}$$

$$[\lambda(t)] = \begin{bmatrix} \lambda_a(t) \\ \lambda_b(t) \\ \lambda_c(t) \\ \lambda_f(t) \\ \lambda_D(t) \\ \lambda_Q(t) \end{bmatrix} \tag{2.1.5}$$

$v_a(t)$, $v_b(t)$, and $v_c(t)$ are the terminal voltages of phase-a winding , phase-b winding, and phase-c winding, respectively.

$v_f(t)$ is the terminal voltage of the field winding.

R_a, R_f, R_D, and R_Q are the resistances of an armature winding, the field winding, the D-damper winding, and the Q-damper winding, respectively.

$i_a(t)$, $i_b(t)$, and $i_c(t)$ are the currents passing through phase-a winding, phase-b winding, and phase-c winding, respectively.

$i_f(t)$, $i_D(t)$, and $i_Q(t)$ are the currents passing through the field winding, the D-damper winding, and the Q-damper winding, respectively.

$\lambda_a(t)$, $\lambda_b(t)$, and $\lambda_c(t)$ are the flux linkages linking phase-a winding, phase-b winding, and phase-c winding, respectively.

$\lambda_f(t)$, $\lambda_D(t)$, and $\lambda_Q(t)$ are the flux linkages linking the field winding, the D-damper winding, and the Q-damper winding, respectively.

All the flux linkages in equation 2.1.5 are defined as follows:

$$[\lambda(t)] = [L(t)][i(t)] \tag{2.2.1}$$

where

$$[L(t)] = \begin{bmatrix} L_{aa}(t) & L_{ab}(t) & L_{ac}(t) & L_{af}(t) & L_{aD}(t) & L_{aQ}(t) \\ L_{ba}(t) & L_{bb}(t) & L_{bc}(t) & L_{bf}(t) & L_{bD}(t) & L_{bQ}(t) \\ L_{ca}(t) & L_{cb}(t) & L_{cc}(t) & L_{cf}(t) & L_{cD}(t) & L_{cQ}(t) \\ L_{fa}(t) & L_{fb}(t) & L_{fc}(t) & L_{ff}(t) & L_{fD}(t) & L_{fQ}(t) \\ L_{Da}(t) & L_{Db}(t) & L_{Dc}(t) & L_{Df}(t) & L_{DD}(t) & L_{DQ}(t) \\ L_{Qa}(t) & L_{Qb}(t) & L_{Qc}(t) & L_{Qf}(t) & L_{QD}(t) & L_{QQ}(t) \end{bmatrix} \tag{2.2.2}$$

2.3 Calculations of the inductances

The inductance matrix [L(t)] in equation 2.2.2 consists of stator self inductances, stator mutual inductances, rotor self inductances, rotor mutual inductances, and stator-rotor mutual inductances. The rotor position does not influence the rotor self and mutual inductances; however, other inductances depend on rotor position. In order to simplify the model, the terms of order 3 and higher in the Fourier series of the inductances are neglected in the inductance calculations. Consequently, the inductances of a three-phase synchronous generator are defined as follows[4]:

(1) stator self inductances:

$$L_{aa}(t) = L_s + L_m \cos[2\theta(t)] \tag{2.3.1}$$

$$L_{bb}(t) = L_s + L_m \cos\left[2\theta(t) - \frac{4\pi}{3}\right] \tag{2.3.2}$$

$$L_{cc}(t) = L_s + L_m \cos\left[2\theta(t) - \frac{2\pi}{3}\right] \tag{2.3.3}$$

where

$\theta(t)$ is the rotor position angle with respect to the magnetic axis of phase-a winding.

L_s is the constant component of the self inductance of an armature winding.

L_m is the amplitude of the second harmonic component of the self inductance of an armature winding.

(2) stator mutual inductances:

$$L_{ab}(t) = -M_s + L_m \cos\left[2\theta(t) - \frac{2\pi}{3}\right] = L_{ba}(t) \tag{2.4.1}$$

$$L_{ac}(t) = -M_s + L_m \cos\left[2\theta(t) - \frac{4\pi}{3}\right] = L_{ca}(t) \tag{2.4.2}$$

$$L_{bc}(t) = -M_s + L_m \cos[2\theta(t)] = L_{cb}(t) \tag{2.4.3}$$

where M_s is the constant component of the mutual inductance between two armature windings.

(3) rotor self inductances

$$L_{ff}(t) = L_f \tag{2.5.1}$$

$$L_{DD}(t) = L_D \tag{2.5.2}$$

$$L_{QQ}(t) = L_Q \tag{2.5.3}$$

where

L_f is the constant amplitude of the self inductance of the field winding.

L_D is the constant amplitude of the self inductance of the D-damper winding.

L_Q is the constant amplitude of the self inductance of the Q-damper winding.

(4) rotor mutual inductances:

$$L_{fD}(t) = M_R = L_{Df}(t) \tag{2.6.1}$$

$$L_{fQ}(t) = 0 = L_{Qf}(t) \tag{2.6.2}$$

$$L_{DQ}(t) = 0 = L_{QD}(t) \tag{2.6.3}$$

where

M_R is the constant mutual inductance between the field winding and the D-damper winding.

(5) stator-rotor mutual inductances:

$$L_{af}(t) = M_f \cos[\theta(t)] = L_{fa}(t) \tag{2.7.1}$$

$$L_{bf}(t) = M_f \cos\left[\theta(t) - \frac{2\pi}{3}\right] = L_{fb}(t) \tag{2.7.2}$$

$$L_{cf}(t) = M_f \cos\left[\theta(t) - \frac{4\pi}{3}\right] = L_{fc}(t) \tag{2.7.3}$$

$$L_{aD}(t) = M_D \cos[\theta(t)] = L_{Da}(t) \tag{2.7.4}$$

$$L_{bD}(t) = M_D \cos\left[\theta(t) - \frac{2\pi}{3}\right] = L_{Db}(t) \tag{2.7.5}$$

$$L_{cD}(t) = M_D \cos\left[\theta(t) - \frac{4\pi}{3}\right] = L_{Dc}(t) \tag{2.7.6}$$

$$L_{aQ}(t) = M_Q \sin[\theta(t)] = L_{Qa}(t) \tag{2.7.7}$$

$$L_{bQ}(t) = M_Q \sin\left[\theta(t) - \frac{2\pi}{3}\right] = L_{Qb}(t) \tag{2.7.8}$$

$$L_{cQ}(t) = M_Q \sin\left[\theta(t) - \frac{4\pi}{3}\right] = L_{Qc}(t) \tag{2.7.9}$$

where

M_f is the amplitude of the mutual inductance between an armature winding and the field winding.

M_D is the amplitude of the mutual inductance between an armature winding and the D-damper winding.

M_Q is the amplitude of the mutual inductance between an armature winding and the Q-damper winding.

Chapter Three

CORRECTIONS ON THE DIFFERENTIAL EQUATIONS

3.1 Introduction

Since the main magnetic path in a generator is a function of time, the reluctance of the path is not constant. The changes of the reluctance of the path also influence the machine's behavior. In this chapter, corrections on the differential equations of the electrical part are made according to the variations of the reluctance of the magnetic path.

3.2 Inclusion of Reluctance Voltages

Figure 3.1 shows the main magnetic flux path in a salient pole three-phase synchronous generator and Figure 3.2 shows the spatial positions of the magnetic axes of the six windings and the axis of the total magnetomotive force in the machine.

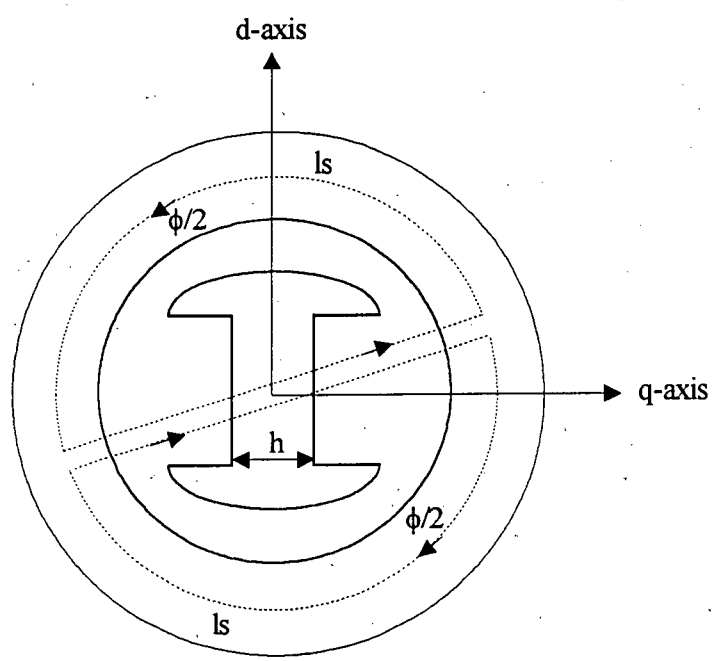

Figure 3.1 Main Magnetic Flux Path of a Salient Pole Three-Phase Synchronous Generator

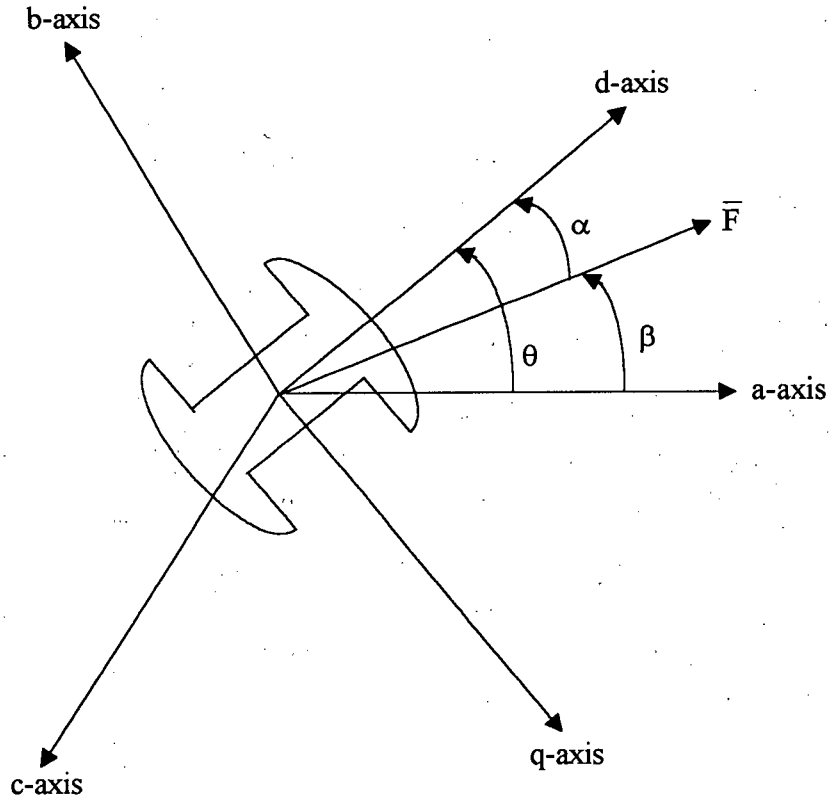

Figure 3.2 Spatial Positions of the Magnetic Axes of the Six Windings and the Axis of the Total Magnetomotive Force

If the flux linkages of the windings are assumed to be the function of the rotor position and the currents only, the flux linkages can be expressed by the following equation:

$$[\lambda(t)] = [\lambda(\theta, i)] \tag{3.1.1}$$

where

$$\theta = \int_{t_o}^{t} \omega(t) \cdot dt \tag{3.1.2}$$

$$i = f(i_a, i_b, i_c, i_f, i_D, i_Q) \tag{3.1.3}$$

$\omega(t)$ is the angular frequency.

Hence, the time derivative of the flux linkage linking each winding becomes:

$$\frac{d}{dt}\lambda_j(t) = \frac{\partial}{\partial\theta}\lambda_j(\theta, i)\frac{d}{dt}\theta + \sum_{k=1}^{6}\frac{\partial}{\partial i_k}\lambda_j(\theta, i)\frac{d}{dt}i_k \tag{3.2}$$

with j = 1, 2, 3, 4, 5, 6 (and k = 1, 2, 3, 4, 5, 6) standing for phase-a winding, phase-b winding, phase-c winding, field winding, D-damper winding, and Q-damper winding, respectively.

By definition, we can also express the flux linkages of the windings as follows:

$$[\lambda(t)] = [L[\theta(t)]][i(t)] \tag{3.3.1}$$

Again, the time derivative of the flux linkage of each winding is given by:

$$\frac{d}{dt}\lambda_j(t) = \sum_{k=1}^{6}\left(L_{jk}[\theta(t)]\frac{d}{dt}i_k(t) + \frac{d}{dt}L_{jk}[\theta(t)]i_k(t)\right) \tag{3.3.2}$$

with j = 1, 2, 3, 4, 5, 6 (and k = 1, 2, 3, 4, 5, 6) standing for phase-a winding, phase-b winding, phase-c winding, field winding, D-damper winding, and Q-damper winding, respectively.

Equation 3.2 and equation 3.3.2 must give the same value of $\frac{d}{dt}\lambda_j(t)$. In deriving equation 3.2 and equation 3.3.2, the variation of the reluctance of the magnetic path with respected to the d-axis is not considered. In a three-phase synchronous generator with a salient pole rotor, the path of the main magnetic flux is a function of time. Thus the mathematical description of the machine needs to be corrected.

Since the main magnetic flux path is varying with time, the flux linkages of the windings should be redefined as follows:

$$[\lambda(t)] = [\lambda(\theta, \alpha, i)] \tag{3.4}$$

where

i is the total current.

α is the angle between the axis of the total magnetomotive force and the d-axis.

By definition, the flux and the flux linkage of each winding have the following relationship:

$$\lambda_j(t) = N_j \Phi_j(\theta, \alpha, i) \tag{3.5.1}$$

where

$$\Phi_j = \Phi(\theta, \alpha, i)\cos\gamma_j \tag{3.5.2}$$

j = 1, 2, 3, 4, 5, 6 standing for phase-a winding, phase-b winding, phase-c winding, field winding, D-damper winding, and Q-damper winding, respectively.

$\Phi(\theta, \alpha, i)$ is the total flux.

$\Phi_j(\theta, \alpha, i)$ is the flux through winding j.

γ_j is the angle between the axis of the total magnetomotive force and the magnetic axis of winding j.

Hence, from equation 3.5.1 and equation 3.5.2 the time derivative of the flux linkage of each individual winding has the following expression:

$$\frac{d}{dt}\lambda_j(t) = v_{L_j}(t) + v_{correction-j}(t) \tag{3.6.1}$$

where

$$\begin{aligned} v_{L_j}(t) = {} & N_j\left[\cos(\gamma_j)\frac{\partial}{\partial\theta}\Phi(\theta, \alpha, i)\frac{d}{dt}\theta\right] \\ & + N_j\left[\cos(\gamma_j)\sum_{k=1}^{6}\frac{\partial}{\partial i_k}\Phi(\theta, \alpha, i)\frac{d}{dt}i_k - \Phi(\theta, \alpha, i)\sin(\gamma_j)\frac{d}{dt}\gamma_j\right] \end{aligned} \tag{3.6.2}$$

$$v_{correction-j}(t) = N_j \cos(\gamma_j) \frac{\partial}{\partial \alpha} \Phi(\theta, \alpha, i) \frac{d}{dt} \alpha \tag{3.6.3}$$

Comparing with equation 3.2 and equation 3.3.2, equation 3.6.1 becomes:

$$\frac{d}{dt} \lambda_j(t) = \frac{d}{dt} \sum_{k=1}^{6} L_{jk}(t) i_k(t) + N_j \cos(\gamma_j) \frac{\partial}{\partial \alpha} \Phi(\theta, \alpha, i) \frac{d}{dt} \alpha \tag{3.7}$$

Hence, equation 2.1.1 should be corrected as follows:

$$[v(t)] = -[R][i(t)] - \frac{d}{dt}[[L(t)][i(t)]] - [v_{rel}(t)] \tag{3.8.1}$$

where

$$[R] = \begin{bmatrix} R_a & 0 & 0 & 0 & 0 & 0 \\ 0 & R_a & 0 & 0 & 0 & 0 \\ 0 & 0 & R_a & 0 & 0 & 0 \\ 0 & 0 & 0 & R_f & 0 & 0 \\ 0 & 0 & 0 & 0 & R_D & 0 \\ 0 & 0 & 0 & 0 & 0 & R_Q \end{bmatrix} \tag{3.8.2}$$

$$[i(t)] = \begin{bmatrix} i_a(t) \\ i_b(t) \\ i_c(t) \\ i_f(t) \\ i_D(t) \\ i_Q(t) \end{bmatrix} \tag{3.8.3}$$

$$[L(t)] = \begin{bmatrix} L_{aa}(t) & L_{ab}(t) & L_{ac}(t) & L_{af}(t) & L_{aD}(t) & L_{aQ}(t) \\ L_{ba}(t) & L_{bb}(t) & L_{bc}(t) & L_{bf}(t) & L_{bD}(t) & L_{bQ}(t) \\ L_{ca}(t) & L_{cb}(t) & L_{cc}(t) & L_{cf}(t) & L_{cD}(t) & L_{cQ}(t) \\ L_{fa}(t) & L_{fb}(t) & L_{fc}(t) & L_{ff}(t) & L_{fD}(t) & L_{fQ}(t) \\ L_{Da}(t) & L_{Db}(t) & L_{Dc}(t) & L_{Df}(t) & L_{DD}(t) & L_{DQ}(t) \\ L_{Qa}(t) & L_{Qb}(t) & L_{Qc}(t) & L_{Qf}(t) & L_{QD}(t) & L_{QQ}(t) \end{bmatrix} \tag{3.8.4}$$

$$[v_{rel}(t)] = \begin{bmatrix} N_a\cos(\beta) \\ N_b\cos\left(\beta - \frac{2\pi}{3}\right) \\ N_c\cos\left(\beta - \frac{4\pi}{3}\right) \\ N_f\cos(\alpha) \\ N_D\cos(\alpha) \\ N_Q\cos\left(\alpha - \frac{\pi}{2}\right) \end{bmatrix} \frac{\partial}{\partial\alpha}\Phi(\theta, \alpha, i)\frac{d}{dt}\alpha \tag{3.8.5}$$

N_a, N_b, N_c, N_f, N_D, and N_Q are the number of turns of phase-a winding, phase-b winding, phase-c winding, field winding, D-damper winding, and Q-damper winding, respectively. From equation 3.8.1 the equivalent circuit of the generator in the continuous time domain is given in Figure 3.3.

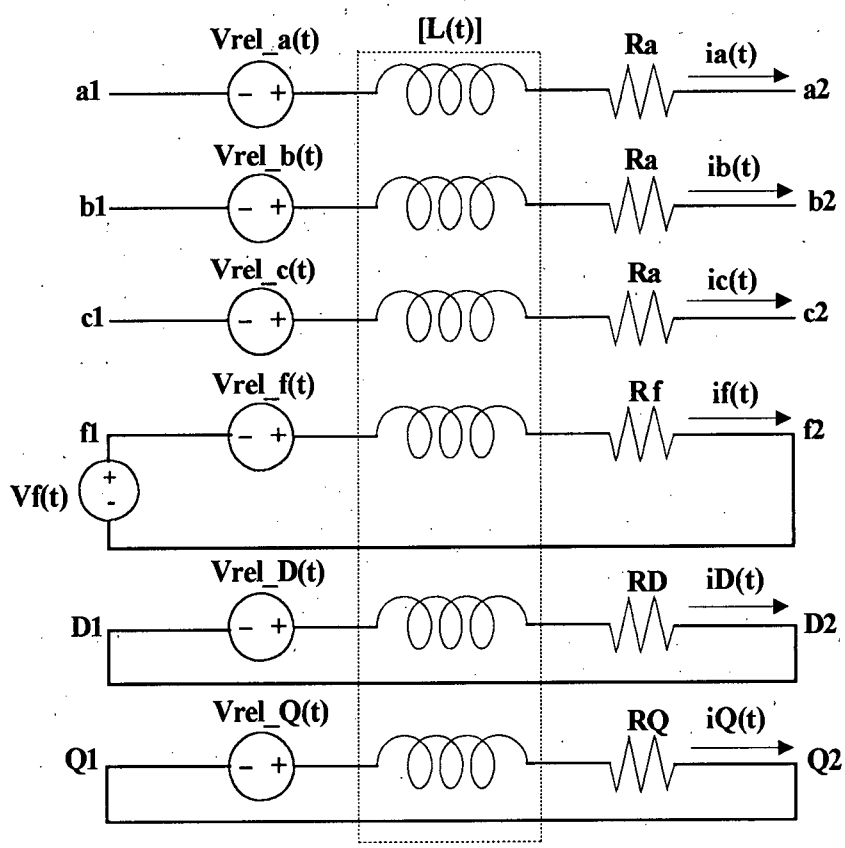

Figure 3.3 Equivalent Circuit of a Salient Pole Three-Phase Synchronous Generator in the Continuous Time Domain

$[v_{rel}(t)]$ is called the reluctance voltage matrix because it is due to the variations of the reluctance of the main magnetic flux path. For salient pole generators, the reluctance voltages exist to account for the changes of the reluctance of the main magnetic flux path. Note that this reluctance voltage term has not been accounted for in dqo analysis.

3.3 Calculations of the Reluctance Voltages

By definition, the total magnetomotive force in the air gap between the rotor and the stator is given by[5]:

$$\vec{F}=\vec{F}_a+\vec{F}_b+\vec{F}_c+\vec{F}_f+\vec{F}_D+\vec{F}_Q \tag{3.9}$$

Where

$\vec{F}_a$, $\vec{F}_b$, $\vec{F}_c$, $\vec{F}_f$, $\vec{F}_D$, and $\vec{F}_Q$ are the magnetomotive forces generated by the currents in phase-a winding, phase-b winding, phase-c winding, field winding, D-damper winding, and Q-damper winding, respectively.

With the magnetic axis of phase-a winding as reference, the total magnetomotive force at any instant t is obtained by the following equation:

$$\vec{F}=\vec{F}_s+\vec{F}_r=F\angle\beta \tag{3.10.1}$$

where

$$\vec{F}_s=N_a i_a(t)\angle 0+N_b i_b(t)\angle\frac{2\pi}{3}+N_c i_c(t)\angle\frac{4\pi}{3} \tag{3.10.2}$$

$$\vec{F}_r=N_f i_f(t)\angle\theta+N_D i_D(t)\angle\theta+N_Q i_Q(t)\angle(\theta-\frac{\pi}{2}) \tag{3.10.3}$$

The real part and the imaginary part of the total magnetomotive force are obtained by the following equations:

$$F_{real}(t)=F_{s\_real}(t)+F_{r\_real}(t) \tag{3.11.1}$$

$$F_{img}(t) = F_{s\_img}(t) + F_{r\_img}(t) \tag{3.11.2}$$

where

$$F_{s\_real}(t) = N_a i_a(t) + N_b i_b(t)\cos\left(\frac{2\pi}{3}\right) + N_c i_c(t)\cos\left(\frac{4\pi}{3}\right) \tag{3.11.3}$$

$$F_{r\_real}(t) = N_f i_f(t)\cos(\theta) + N_D i_D(t)\cos(\theta) + N_Q i_Q(t)\cos\left(\theta - \frac{\pi}{2}\right) \tag{3.11.4}$$

$$F_{s\_img}(t) = N_b i_b(t)\sin\left(\frac{2\pi}{3}\right) + N_c i_c(t)\sin\left(\frac{4\pi}{3}\right) \tag{3.11.5}$$

$$F_{r\_img}(t) = N_f i_f(t)\sin(\theta) + N_D i_D(t)\sin(\theta) + N_Q i_Q(t)\sin\left(\theta - \frac{\pi}{2}\right) \tag{3.11.6}$$

Consequently, the amplitude and the angle of the total magnetomotive force are given by the following equations:

$$F = \sqrt{F_{real}^2(t) + F_{img}^2(t)} \tag{3.12.1}$$

$$\beta(t) = \arctan\left(\frac{F_{img}(t)}{F_{real}(t)}\right) \tag{3.12.2}$$

Once $\theta(t)$ and $\beta(t)$ are known, $\alpha(t)$ can be calculated by:

$$\alpha(t) = \theta(t) - \beta(t) \tag{3.13}$$

Since $\Phi(\theta,\alpha,i)$ is the total magnetic flux passing through the main magnetic flux path, its value should be obtained from the available magnetizing curves. Figure 3.4 outlines the procedure to generate the curves of $\Phi(\theta,\alpha,i)$ vs α from the magnetizing curves in the un-saturated case.

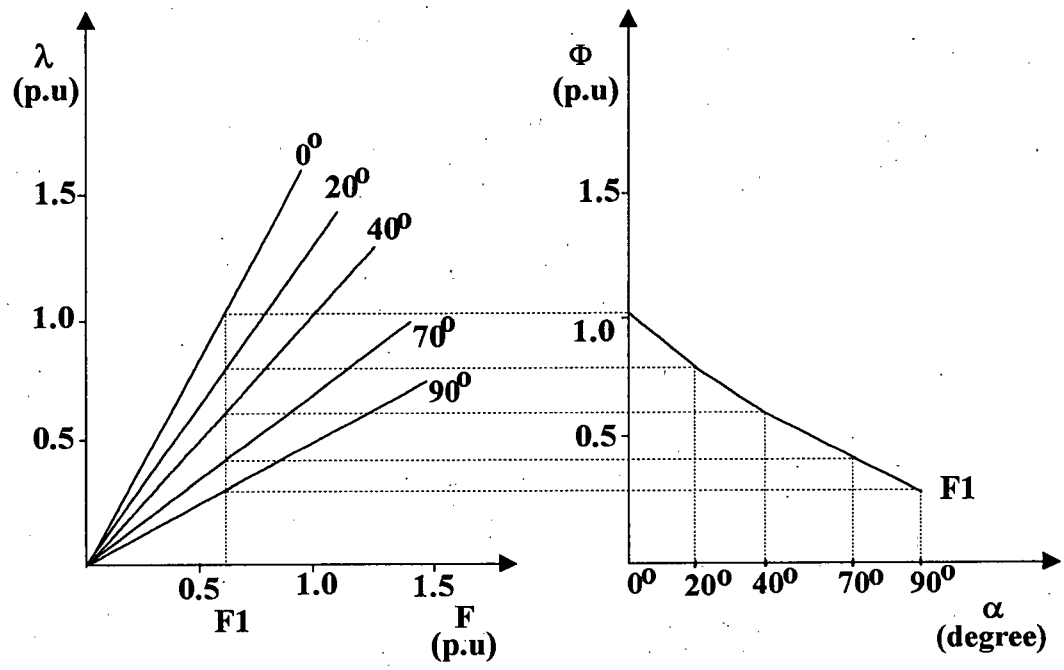

Figure 3.4 Development of the Curves of $\Phi(\theta,\alpha,i)$ vs α

According to the magnetizing curves, the total flux and flux linkage of the six magnetically coupled windings have the following relationship:

$$\Phi(\theta,\alpha,i) = \frac{\lambda(\theta,\alpha,i)}{N_a} \tag{3.14}$$

Therefore, the partial derivative of the total magnetic flux with respect to α is given by:

$$\frac{\partial}{\partial\alpha}\Phi(\theta,\alpha,i) = \frac{1}{N_a}\frac{\partial}{\partial\alpha}\lambda(\theta,\alpha,i) \tag{3.15}$$

Assuming that each phase winding has the same number of turns, from equations 3.8.5 and 3.15 the reluctance voltages can be calculated as:

$$[v_{rel}(t)] = \begin{bmatrix} \cos(\beta) \\ \cos\left(\beta - \frac{2\pi}{3}\right) \\ \cos\left(\beta - \frac{4\pi}{3}\right) \\ \frac{N_f}{N_a}\cos(\alpha) \\ \frac{N_D}{N_a}\cos(\alpha) \\ \frac{N_Q}{N_a}\cos\left(\alpha - \frac{\pi}{2}\right) \end{bmatrix} \frac{\partial}{\partial\alpha}\lambda(\theta, \alpha, i)\frac{d}{dt}\alpha \tag{3.16}$$

Chapter Four

MATHEMATICAL DESCRIPTION OF THE MECHANICAL PART

4.1 Introduction

The mechanical part of a three-phase synchronous generator consists mainly of a rotor core, a turbine (or turbines), and an exciter machine mass. The turbine (or turbines) and the exciter machine mass are attached to the shaft of the rotor of the generator. When the generator is in operation, high pressure steam or water jets strike the turbine blades, forcing the rotor to rotate rapidly. The mechanical part of the generator is used to input mechanical power to the machine and its dynamic behavior affects the machine's performance. In this chapter, the differential equations of the mechanical part of a three-phase synchronous generator are derived based on the assumption that the masses mounted to the shaft of the rotor are rigid bodies.

4.2 Differential Equations of the Mechanical Part

Figure 4.1 shows a schematic of the mechanical part of a three-phase synchronous generator[6].

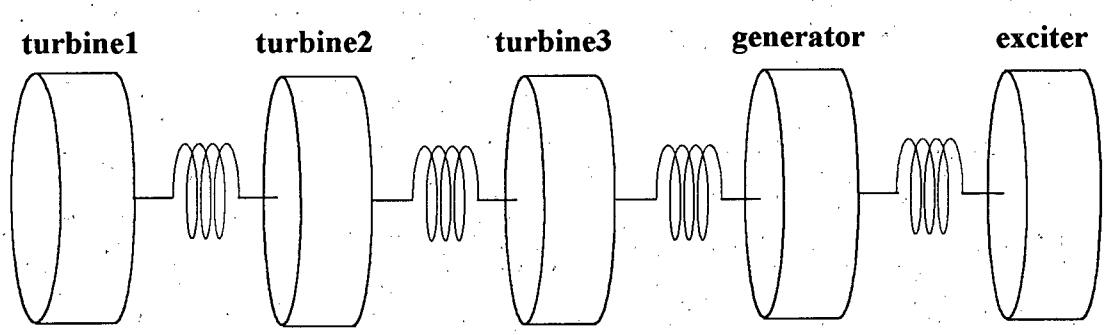

Figure 4.1 Mechanical Part of a Three-Phase Synchronous Generator

In operation, a three-phase synchronous generator experiences forces on its shaft. The total torque on the shaft consists of the mechanical torque and the electrical torque. The former is the externally applied torque and the latter is the torque generated by the interactions of the magnetic fields. The total torque can be expressed as follows:

$$[T(t)] = [T_m(t)] - [[T_g(t)] + [T_{exciter}(t)]] \tag{4.1}$$

where [T(t)] is the total torque, $[T_m(t)]$ is the mechanical torque input to the turbine (or turbines), $[T_g(t)]$ is the electromagnetic torque of the generator, and $[T_{exciter}(t)]$ is the electromagnetic torque of the exciter machine mounted to the shaft of the rotor.

According to the analogue of Newton's second law for angular motion, the mechanical part of the machine can be represented by the following differential equation[7,8]:

$$[J_m]\frac{d^2}{dt^2}[\theta_m] + [D_m]\frac{d}{dt}[\theta_m] + [K_m][\theta_m] = [T(t)] \tag{4.2.1}$$

where

m is the subscript standing for the mechanical side of the generator.

$[J_m]$ is the diagonal matrix of the moment of inertia of the masses mounted to the shaft of the rotor.

$[\theta_m]$ is the diagonal matrix of the position angles of the masses mounted to the shaft of the rotor.

$[D_m]$ is the tridiagonal matrix of the damping coefficients of the fluid around the masses.

$[K_m]$ is the tridiagonal matrix of the stiffness coefficients of the amortisseure springs between the different masses mounted to the shaft of the rotor.

[T(t)] is the vector of the total torque on the shaft of the rotor.

Explicitly, we have $[J_m]$, $[\theta_m]$, $[D_m]$, $[K_m]$, and [T(t)] as follows:

$$[J_m] = \begin{bmatrix} J_1 & 0 & \cdots & \cdots & 0 \\ 0 & J_2 & 0 & \cdots & 0 \\ \cdots & \cdots & \cdots & \cdots & \cdots \\ 0 & \cdots & 0 & J_{n-1} & 0 \\ 0 & \cdots & \cdots & 0 & J_n \end{bmatrix} \tag{4.2.2}$$

$$[\theta_m] = \begin{bmatrix} \theta_1 \\ \theta_2 \\ \cdots \\ \theta_{n-1} \\ \theta_n \end{bmatrix} \tag{4.2.3}$$

$$[D_m] = \begin{bmatrix} D_1 + D_2 & -D_{12} & 0 & \cdots & \cdots & 0 \\ -D_{12} & D_{12} + D_2 + D_{23} & -D_{23} & 0 & \cdots & 0 \\ \cdots & \cdots & \cdots & \cdots & \cdots & \cdots \\ 0 & \cdots & \cdots & 0 & D_{n-1,n} & D_{n-1,n} + D_n \end{bmatrix} \tag{4.2.4}$$

$$[K_m] = \begin{bmatrix} K_{12} & -K_{12} & 0 & \cdots & \cdots & 0 \\ -K_{12} & K_{12} + K_{23} & -K_{23} & 0 & \cdots & 0 \\ \cdots & \cdots & \cdots & \cdots & \cdots & \cdots \\ 0 & \cdots & \cdots & 0 & -K_{n-1,n} & K_{n-1,n} \end{bmatrix} \tag{4.2.5}$$

$$[T(t)] = \begin{bmatrix} T_1(t) \\ \cdots \\ \cdots \\ \cdots \\ T_n(t) \end{bmatrix} = \begin{bmatrix} T_{turbine\_1}(t) \\ \cdots \\ T_{turbine\_s}(t) \\ 0 \\ 0 \end{bmatrix} - \left[\begin{bmatrix} 0 \\ \cdots \\ 0 \\ T_{ge}(t) \\ 0 \end{bmatrix} + \begin{bmatrix} 0 \\ \cdots \\ 0 \\ 0 \\ T_{exc}(t) \end{bmatrix} \right] \tag{4.2.6}$$

where

s is the number of turbines mounted to the shaft of the rotor.

$T_{turbine\_s}(t)$ is the mechanical torque input to turbine s.

$T_{ge}(t)$ is the electromagnetic torque of the generator exerted on the shaft of the rotor.

$T_{exc}(t)$ is the electromagnetic torque of the exciter machine exerted on the shaft of the rotor.

Equation 4.2.1 can be represented on the electrical side as well and the conversion between the machine quantities on the mechanical side and those on the electrical side is done by the following relationships:

$$[J_e] = \frac{[J_m]}{\left(\frac{p}{2}\right)^2} \tag{4.3.1}$$

$$[\theta_e(t)] = \left(\frac{p}{2}\right)[\theta_m(t)] \tag{4.3.2}$$

$$[D_e] = \frac{[D_m]}{\left(\frac{p}{2}\right)^2} \tag{4.3.3}$$

$$[k_e] = \frac{[k_m]}{\left(\frac{p}{2}\right)^2} \tag{4.3.4}$$

$$[T_e(t)] = \frac{[T_m(t)]}{\left(\frac{p}{2}\right)} \tag{4.3.5}$$

where

the subscript e stands for the electrical side of the generator.

the subscript m stands for the mechanical side of the generator.

p is the number of poles of the generator.

4.3 Calculations of the Electrical Torques

The electrical torques on the shaft by the generator and the exciter are derived in different manners. $[T_g(t)]$ can be derived using the principle of conservation of instantaneous power. Let $p_e(t)$ be the electrical power generated by the generator at time t, $p_e(t)$ is expressed as[9]:

$$p_e(t) = [i(t)]^T[R][i(t)] + [i(t)]^T[L(\theta)]\left(\frac{d}{dt}[i(t)]\right) + [i(t)]^T\left(\frac{d}{dt}[L(\theta)]\right)[i(t)] \quad (4.4)$$

The instantaneous stored magnetic energy of the magnetically coupled coils is given by:

$$W(t) = \frac{1}{2}[i(t)]^T[L(\theta)][i(t)] \quad (4.5)$$

Differentiating both sides of equation 4.5 gives the following expression for the power obtained from the magnetic field:

$$\frac{d}{dt}W(t) = \frac{1}{2}[i(t)]^T[L(\theta)]\frac{d}{dt}[i(t)] + \frac{1}{2}\frac{d}{dt}[i(t)]^T[L(\theta)][i(t)]$$
$$+\frac{1}{2}[i(t)]^T\frac{d}{dt}[L(\theta)][i(t)] \quad (4.6)$$

Since the transpose of a product of matrices is the product of the transposed matrices in reverse order and $[L(\theta)]$ is a symmetric matrix, the following equation holds:

$$\frac{1}{2}\frac{d}{dt}[i(t)]^T[L(\theta)][i(t)] = \frac{1}{2}[i(t)]^T[L(\theta)]\frac{d}{dt}[i(t)] \quad (4.7)$$

Combining equations 4.6 and 4.7 gives:

$$\frac{d}{dt}W(t) = [i(t)]^T[L(\theta)]\left(\frac{d}{dt}[i(t)]\right) + \frac{1}{2}[i(t)]^T\left(\frac{d}{dt}[L(\theta)]\right)[i(t)] \quad (4.8)$$

From equations 4.4 and 4.8, the instantaneous power generated can be rewritten as follows:

$$p_e(t) = [i(t)]^T[R][i(t)] + \frac{d}{dt}W(t) + \frac{1}{2}[i(t)]^T\left(\frac{d}{dt}[L(\theta)]\right)[i(t)] \tag{4.9}$$

Equation 4.9 indicates that electrical power generated consists three components: power dissipated in resistances of the windings, power in the magnetic fields, and power converted into mechanical form. The electrical power converted into mechanical form is given by:

$$p_{ge}(t) = \frac{1}{2}[i(t)]^T\frac{d}{dt}[L(\theta)][i(t)] = \omega T_{ge}(t) \tag{4.10}$$

Applying the chain rule in calculus on [L(θ)] gives the following equation:

$$\frac{d}{dt}[L(\theta)] = \frac{d}{d\theta}[L(\theta)]\frac{d\theta}{dt} \tag{4.11}$$

Since dθ/dt is the angular velocity, from equations 4.10 and 4.11, the electrical torque of the generator on the shaft is given by:

$$T_{ge}(t) = \frac{1}{2}[i(t)]^T\left(\frac{d}{d\theta}[L(\theta)]\right)[i(t)] \tag{4.12.1}$$

Since there is only one generator mass, equation 4.12.1 can be put into a vector form as follows:

$$[T_g(t)] = \begin{bmatrix} 0 \\ \cdots\cdots \\ 0 \\ T_{ge}(t) \\ 0 \end{bmatrix} \tag{4.12.2}$$

When the field winding is excited by an exciter machine mounted on the shaft of the rotor, the torque applied on the shaft by the exciter machine must be considered. In operation, the power input to the exciter machine from the turbine (or turbines) is:

$$p_{exc}(t) = T_{exc}(t)\omega_m \tag{4.13}$$

where $\omega_m(t)$ is the rotational speed of exciter machine mass.

By the law of conservation of energy, the power of the exciter machine obtained from the turbine (or turbines) is given by:

$$p_{exc}(t) = -v_f(t)i_f(t) + i_f(t)R_{exc} \tag{4.14}$$

From equations 4.13 and 4.14 the torque exerted on the shaft of the rotor by the exciter machine becomes:

$$T_{exc}(t) = \frac{-v_f(t)i_f(t) + i_f(t)R_{exc}}{\omega_m} \tag{4.15}$$

where R_{exc} is the resistance of the winding of the exciter machine.

Since there is only one exciter machine mass, the electrical torque of the exciter machine can be also put into a vector form:

$$[T_{exciter}(t)] = \begin{bmatrix} 0 \\ \cdots\cdots \\ 0 \\ 0 \\ T_{exc}(t) \end{bmatrix}. \tag{4.16}$$

Chapter Five

DISCRETE-TIME MODEL OF THE GENERATOR

5.1 Introduction

Once the differential equations of a three-phase synchronous generator are available, they should be solved such that the machine's behaviour can be analyzed. These equations can be solved in either the frequency domain or the time domain which is used in the model development. In order to create a computer simulation program for a three-phase synchronous generator, the differential equations of the machine need to be discretized with some integration rule. In this chapter, the discrete-time model of a three-phase synchronous generator is developed using the trapezoidal rule of integration. The link between the electrical and mechanical parts is the rotor position angle and the electromagnetic torques exerted on the shaft of the rotor by both the generator and the exciter machine.

5.2 Discrete-Time Model of the Electrical Part

To solve the machine's electrical quantities in the time domain, equation 3.8.1 is discretized by the trapezoidal integration rule, resulting in the following equation[10]:

$$\begin{bmatrix} [v_1(t)] \\ [v_2(t)] \end{bmatrix} = -\frac{2}{\Delta t}\begin{bmatrix} [R_1(t)] & [R_2(t)] \\ [R_3(t)] & [R_4(t)] \end{bmatrix}\begin{bmatrix} [i_1(t)] \\ [i_2(t)] \end{bmatrix} - \frac{2}{\Delta t}\begin{bmatrix} [v_{rel1}(t)] \\ [v_{rel2}(t)] \end{bmatrix} + \begin{bmatrix} [e_{1h}(t)] \\ [e_{2h}(t)] \end{bmatrix} \tag{5.1.1}$$

where

$$[v_1(t)] = \begin{bmatrix} v_a(t) \\ v_b(t) \\ v_c(t) \end{bmatrix} \tag{5.1.2}$$

$$[v_2(t)] = \begin{bmatrix} v_f(t) \\ 0 \\ 0 \end{bmatrix} \tag{5.1.3}$$

$$[i_1(t)] = \begin{bmatrix} i_a(t) \\ i_b(t) \\ i_c(t) \end{bmatrix} \tag{5.1.4}$$

$$[i_2(t)] = \begin{bmatrix} i_f(t) \\ i_D(t) \\ i_Q(t) \end{bmatrix} \tag{5.1.5}$$

$$[R_1(t)] = \frac{\Delta t}{2}\begin{bmatrix} R_a & 0 & 0 \\ 0 & R_a & 0 \\ 0 & 0 & R_a \end{bmatrix} + \begin{bmatrix} L_{aa}(t) & L_{ab}(t) & L_{ac}(t) \\ L_{ba}(t) & L_{bb}(t) & L_{bc}(t) \\ L_{ca}(t) & L_{cb}(t) & L_{cc}(t) \end{bmatrix} \tag{5.1.6}$$

$$[R_2(t)] = \begin{bmatrix} L_{af}(t) & L_{aD}(t) & L_{aQ}(t) \\ L_{bf}(t) & L_{bD}(t) & L_{bQ}(t) \\ L_{cf}(t) & L_{cD}(t) & L_{cQ}(t) \end{bmatrix} \tag{5.1.7}$$

$$[R_3(t)] = \begin{bmatrix} L_{fa}(t) & L_{fb}(t) & L_{fc}(t) \\ L_{Da}(t) & L_{Db}(t) & L_{Dc}(t) \\ L_{Qa}(t) & L_{Qb}(t) & L_{Qc}(t) \end{bmatrix} \tag{5.1.8}$$

$$[R_4(t)] = \frac{\Delta t}{2}\begin{bmatrix} R_f & 0 & 0 \\ 0 & R_D & 0 \\ 0 & 0 & R_Q \end{bmatrix} + \begin{bmatrix} L_{ff}(t) & L_{fD}(t) & L_{fQ}(t) \\ L_{Df}(t) & L_{DD}(t) & L_{DQ}(t) \\ L_{Qf}(t) & L_{QD}(t) & L_{QQ}(t) \end{bmatrix} \tag{5.1.9}$$

$$[v_{rel1}(t)] = \frac{2}{\Delta t}\begin{bmatrix} \cos[\beta(t)] \\ \cos\left[\beta(t) - \frac{2\pi}{3}\right] \\ \cos\left[\beta(t) - \frac{4\pi}{3}\right] \end{bmatrix} \frac{\partial}{\partial \alpha}\lambda(\theta, \alpha, i)\alpha(t) \tag{5.1.10}$$

$$[v_{rel2}(t)] = \frac{2}{\Delta t}\begin{bmatrix} \frac{N_f}{N_a}\cos[\alpha(t)] \\ \frac{N_D}{N_a}\cos[\alpha(t)] \\ \frac{N_Q}{N_a}\cos\left[\alpha(t) - \frac{\pi}{2}\right] \end{bmatrix} \frac{\partial}{\partial \alpha}\lambda(\theta, \alpha, i)\alpha(t) \tag{5.1.11}$$

$$[R_1(t-\Delta t)] = -\frac{\Delta t}{2}\begin{bmatrix} R_a & 0 & 0 \\ 0 & R_a & 0 \\ 0 & 0 & R_a \end{bmatrix} + \begin{bmatrix} L_{aa}(t-\Delta t) & L_{ab}(t-\Delta t) & L_{ac}(t-\Delta t) \\ L_{ba}(t-\Delta t) & L_{bb}(t-\Delta t) & L_{bc}(t-\Delta t) \\ L_{ca}(t-\Delta t) & L_{cb}(t-\Delta t) & L_{cc}(t-\Delta t) \end{bmatrix} \tag{5.1.12}$$

$$[R_2(t-\Delta t)] = \begin{bmatrix} L_{af}(t-\Delta t) & L_{aD}(t-\Delta t) & L_{aQ}(t-\Delta t) \\ L_{bf}(t-\Delta t) & L_{bD}(t-\Delta t) & L_{bQ}(t-\Delta t) \\ L_{cf}(t-\Delta t) & L_{cD}(t-\Delta t) & L_{cQ}(t-\Delta t) \end{bmatrix} \tag{5.1.13}$$

$$[R_3(t-\Delta t)] = \begin{bmatrix} L_{fa}(t-\Delta t) & L_{fb}(t-\Delta t) & L_{fc}(t-\Delta t) \\ L_{Da}(t-\Delta t) & L_{Db}(t-\Delta t) & L_{Dc}(t-\Delta t) \\ L_{Qa}(t-\Delta t) & L_{Qb}(t-\Delta t) & L_{Qc}(t-\Delta t) \end{bmatrix} \tag{5.1.14}$$

$$[R_4(t-\Delta t)] = -\frac{\Delta t}{2}\begin{bmatrix} R_f & 0 & 0 \\ 0 & R_D & 0 \\ 0 & 0 & R_Q \end{bmatrix} + \begin{bmatrix} L_{ff}(t-\Delta t) & L_{fD}(t-\Delta t) & L_{fQ}(t-\Delta t) \\ L_{Df}(t-\Delta t) & L_{DD}(t-\Delta t) & L_{DQ}(t-\Delta t) \\ L_{Qf}(t-\Delta t) & L_{QD}(t-\Delta t) & L_{QQ}(t-\Delta t) \end{bmatrix} \tag{5.1.15}$$

$$[e_{1ha}(t)] = \frac{2}{\Delta t}([R_1(t-\Delta t)][i_1(t-\Delta t)] + [R_2(t-\Delta t)][i_2(t-\Delta t)]) - [v_1(t-\Delta t)] \tag{5.1.16}$$

$$[e_{2ha}(t)] = \frac{2}{\Delta t}([R_3(t-\Delta t)][i_1(t-\Delta t)] + [R_4(t-\Delta t)][i_2(t-\Delta t)]) - [v_2(t-\Delta t)] \tag{5.1.17}$$

$$[e_{1hb}(t)] = \frac{2}{\Delta t}\begin{bmatrix} \cos[\beta(t-\Delta t)] \\ \cos\left[\beta(t-\Delta t) - \frac{2\pi}{3}\right] \\ \cos\left[\beta(t-\Delta t) - \frac{4\pi}{3}\right] \end{bmatrix} \frac{\partial}{\partial\alpha}\lambda[\theta(t-\Delta t), \alpha(t-\Delta t), i(t-\Delta t)]\alpha(t-\Delta t) \tag{5.1.18}$$

$$[e_{2hb}(t)] = \frac{2}{\Delta t}\begin{bmatrix} \frac{N_f}{N_a}\cos[\alpha(t-\Delta t)] \\ \frac{N_D}{N_a}\cos\left[\alpha(t-\Delta t) - \frac{2\pi}{3}\right] \\ \frac{N_Q}{N_a}\cos\left[\alpha(t-\Delta t) - \frac{4\pi}{3}\right] \end{bmatrix} \frac{\partial}{\partial\alpha}\lambda[\theta(t-\Delta t), \alpha(t-\Delta t), i(t-\Delta t)]\alpha(t-\Delta t) \tag{5.1.19}$$

$$[e_{1h}(t)] = [e_{1ha}(t)] + [e_{1hb}(t)] \tag{5.1.20}$$

$$[e_{2h}(t)] = [e_{2ha}(t)] + [e_{2hb}(t)] \tag{5.1.21}$$

From equation 5.1.1, the terminal voltages $[v_1(t)]$ and currents $[i_1(t)]$ of the armature windings can be expressed in terms of the terminal voltages $[v_2(t)]$ and currents $[i_2(t)]$ of the field structure windings as follows:

$$[v_1(t)] = -[R_{equ}(t)][i_1(t)] + [e_1(t)] \tag{5.2.1}$$

where

$$[R_{equ}(t)] = \frac{2}{\Delta t}\Big([R_1(t)] - [R_2(t)][R_4(t)]^{-1}[R_3(t)]\Big) \tag{5.2.2}$$

$$[e_{1a}(t)] = \frac{2}{\Delta t}\left([R_2(t)][R_4(t)]^{-1}[v_{rel2}(t)] - [v_{rel1}(t)]\right) \tag{5.2.3}$$

$$[e_{1b}(t)] = [R_2(t)][R_4(t)]^{-1}([v_2(t)] - [e_{2h}(t)]) \tag{5.2.4}$$

$$[e_1(t)] = [e_{1a}(t)] + [e_{1b}(t)] + [e_{1h}(t)] \tag{5.2.5}$$

From equation 5.2.1, the equivalent circuit of the three-phase synchronous generator in the discrete-time domain is obtained as shown in Figure 5.1.

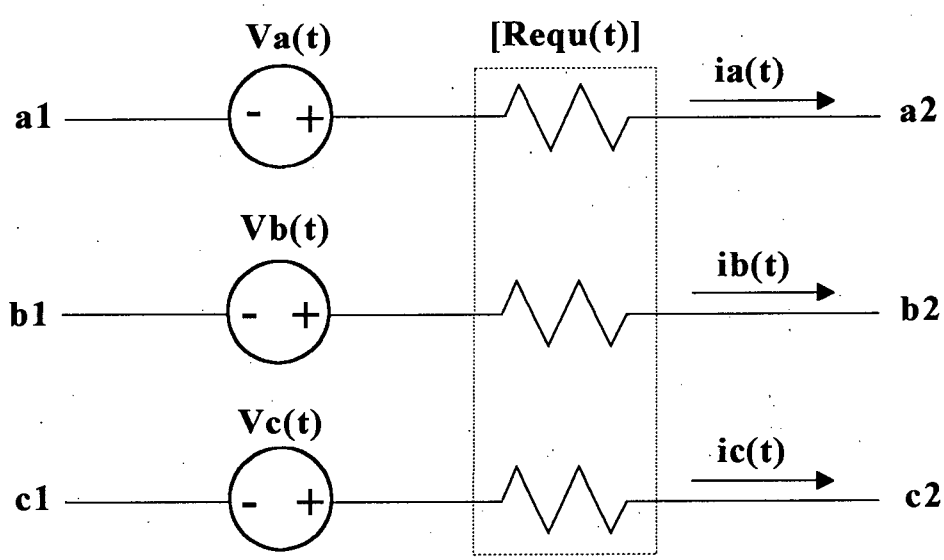

Figure 5.1 Equivalent Circuit of a Salient Pole Three-Phase Synchronous Generator in the Discrete-Time Domain

5.3 Discrete-Time Mode of the Mechanical Part

The differential equations of the generator's mechanical part also have to be discretized so that they can be solved together with the electrical equations in the time domain. By definition, the angular speed of the rotor rotation is given by:

$$[\omega_m(t)] = \frac{d}{dt}[\theta_m(t)] \tag{5.3.1}$$

Discretizing equation 5.3.1 with the trapezoidal rule of integration produces the following relationship between $\omega_m(t)$ and $\theta_m(t)$:

$$\theta_m(t) = \frac{\Delta t}{2}\omega_m(t) + \frac{\Delta t}{2}\omega_m(t-\Delta t) + \theta_m(t-\Delta t) \tag{5.3.2}$$

Applying the trapezoidal rule of integration to equation 4.2.1 and solving for the angular frequency results in the following equation:

$$[\omega_m(t)] = [A]^{-1}\left([B(t)][\omega_m(t-\Delta t)] + \Delta t[k_m][\theta_m(t-\Delta t)] + \frac{\Delta t}{2}[T(t-\Delta t)]\right) \tag{5.4.1}$$

where

$$[A] = [J_m] + \frac{\Delta t}{2}[D_m] + \left(\frac{\Delta t}{2}\right)^2[k_m] \tag{5.4.2}$$

$$[B(t)] = \frac{\Delta t}{2}[T(t)] - \left([J_m] - \frac{\Delta t}{2}[D_m] - \left(\frac{\Delta t}{2}\right)^2[k_m]\right) \tag{5.4.3}$$

To determine the electromagnetic torques of the generator and exciter, the rotor position θ_m at time t is needed. However, since the expressions defining the torque, equation 4.2.1, are quadratic on the currents, an exact solution would require iterations. Iterations can be avoided if $\theta_m(t)$ is predicted. Linear extrapolation can be applied to predict the rotor position angle from the values at two previous solution points:

$$[\theta_m(t)] = 2[\theta_m(t-\Delta t)] - [\theta_m(t-2\Delta t)] \tag{5.5}$$

Since the changes in mechanical quantities are much slower than those of the electrical quantities, the prediction of the rotor position does not introduce significant errors in the simulation results.

Chapter Six

INCLUSION OF MAGNETIC SATURATION EFFECTS

6.1 Introduction

The saturation of magnetic paths also influences the performance of a three-phase synchronous generator. There are different ways to model saturation effects in a generator; however, a much simpler and direct method is possible when the machine equations are written in the phase-domain than in dqo co-ordinates.

6.2 Preliminary Considerations of Magnetic Saturation Effects

The following assumptions are considered acceptable in considering saturation in a synchronous machine[11,12,13]:

(1) The total flux linkages of each magnetically coupled coil are the sum of the leakage flux linkages and the common mutual flux linkages.

(2) The magnetic saturation depends on the total air gap flux linkages.

(3) The leakage fluxes are not subject to magnetic saturation.

(4) The inductances of the magnetically coupled windings maintain their sinusoidal dependence on the rotor position.

(5) Hysteresis and eddy current effects are neglected.

Normally, the only available data of magnetic saturation of a generator is the magnetizing curves. Figure 6.1 shows the magnetizing curves on the d-axis and the q-axis of a typical generator[14].

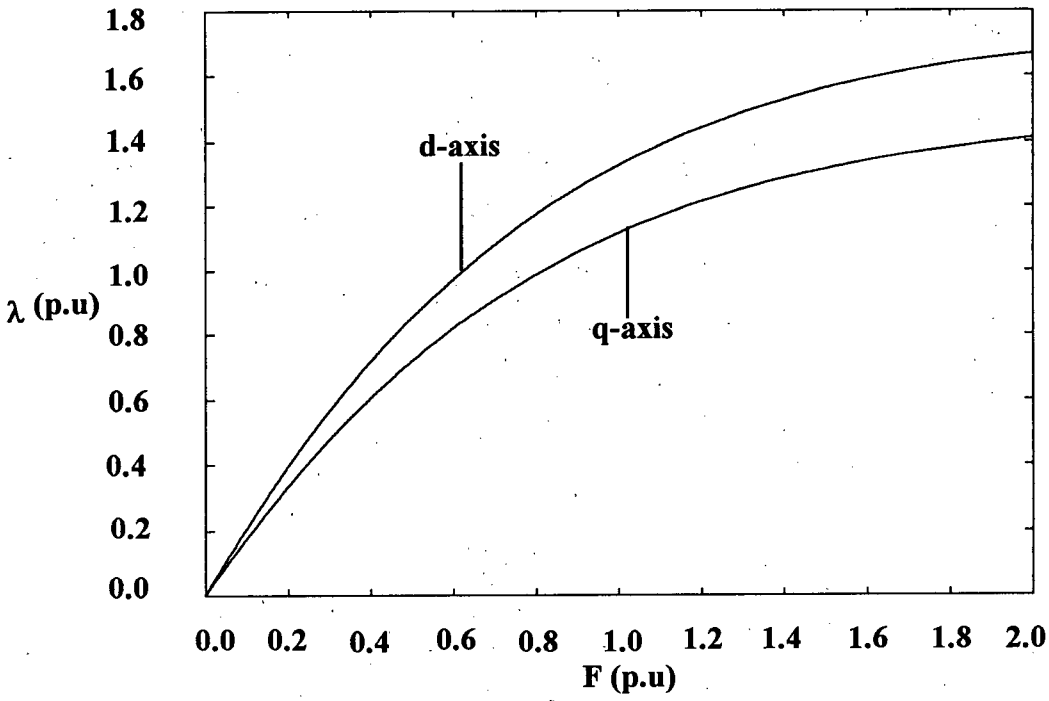

Figure 6.1 Magnetizing Curves on the d-axis and the q-axis of a Three-Phase Synchronous Generator

The saturation curves indicate the relationship between the total flux linkages and the total magnetizing current (or the total magnetomotive force). It is convenient for the analysis that follows to represent the magnetizing curves by analytical functions. Different functions can be used to approximate the saturation curves but one of the most accurate methods is to use proper polynomials. A polynomial function of degree n has the following general form[15]:

$$p(x) = a_o + a_1 x + a_2 x^2 + \ldots + a_n x^n \tag{6.1}$$

where a_o, a_1, a_2, ... a_n are the coefficients of the polynomial.

In order to represent a given saturation curve along a given air gap position, a set of magnetizing current (or total magnetomotive force) values versus the corresponding flux

linkages is needed. The number of the data points must be at least equal to the degree of the chosen polynomial. From the given data points, a system of equations can be set up to satisfy equation 6.1:

$$\begin{bmatrix} \lambda_1(i_{m\_1}) \\ \cdots\cdots\cdots \\ \lambda_n(i_{m\_n}) \end{bmatrix} = \begin{bmatrix} a_o & a_1 & a_2 & \ldots & a_n \\ \ldots & \ldots & \ldots & \ldots & \ldots \\ a_o & a_1 & a_2 & \ldots & a_n \end{bmatrix} \begin{bmatrix} i_{m\_1} \\ \cdots\cdots \\ i_{m\_n} \end{bmatrix} \tag{6.2}$$

where

$\lambda_n(i_{m\_n})$ is the flux linkage corresponding to the magnetizing current i_{m_n}.

Solving system 6.2 for the coefficients gives the approximating saturation curve. Since the magnetizing curves are continuous and smooth, using polynomials to fit the curves results in accurate approximations. The fitting of the curves is simple and not time consuming with some available polynomial problem solver program.

6.3 Generation of Magnetic Saturation Curves

Since during transient conditions flux path in a three-phase synchronous generator with a salient pole rotor is changing with time, the magnetizing curves are also dependent on time. To include all possible flux path directions, a number of magnetizing curves should be provided. If only the magnetizing curves in the d-axis and the q-axis are available, other curves may be generated with some approximating techniques[16].

The reluctance of the flux path depends on the lengths of the air gap, the rotor core path, and the stator core path. Figure 6.2 shows all these paths in a generator.

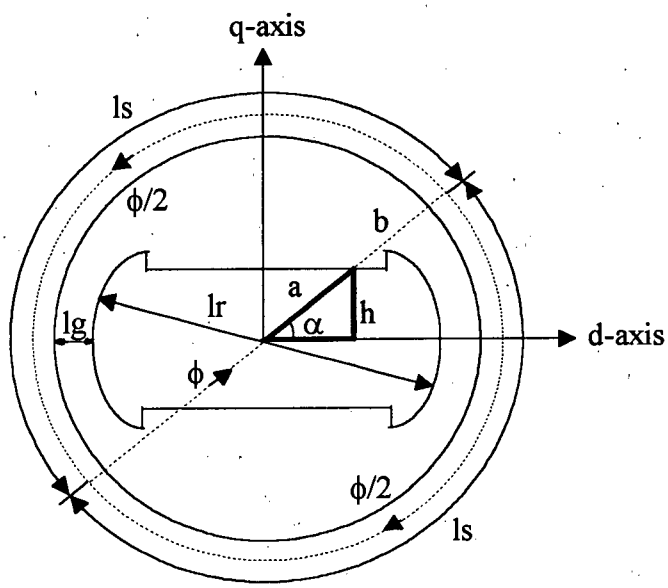

Figure 6.2 Lengths of the Different Sections in the Flux Path

By definition, from Figure 6.2 the reluctance of the main magnetic flux path for a given angle α can be expressed as follows:

$$R_{rel}(\alpha) = R_{rel\_rotor}(\alpha) + R_{rel\_air-gap}(\alpha) + R_{rel\_stator}(\alpha) \tag{6.3.1}$$

where

$$R_{rel\_rotor}(\alpha) = \frac{2a}{\mu_o \mu_r A} = \frac{\frac{2h}{|\sin(\alpha)|}}{\mu_o \mu_r A} \tag{6.3.2}$$

$$R_{rel\_air-gap}(\alpha) = \frac{2b}{\mu_o A} = \frac{l_r + 2l_g - \frac{2h}{|\sin(\alpha)|}}{\mu_o A} \tag{6.3.3}$$

$$R_{rel\_stator}(\alpha) = \frac{l_s}{2\mu_o \mu_r A} \tag{6.3.4}$$

$R_{rel\_rotor}(\alpha)$ is the reluctance of the rotor core path.

$R_{rel\_air-gap}(\alpha)$ is the reluctance of the air gap path.

$R_{rel\text{-}stator}(\alpha)$ is the reluctance of the stator core path.

μ_o is the permeability of the air gap.

μ_r is the relative permeability of the core material of the rotor and the stator.

2a is the length of the rotor core in the main magnetic flux path.

2b is the total air gap in the main magnetic flux path.

A is the cross section area of the main magnetic flux path.

l_r is the length of the rotor core on d-axis.

l_g is the air gap on the d-axis.

l_s is the magnetic path through the stator core.

h is the width of the rotor on the q-axis.

From Figure 6.2 it is clear that the reluctance of the main magnetic flux path has a constant value for some values of α as follows:

$$R_{rel}(\alpha) = \frac{l_r}{\mu_o \mu_r A} + \frac{2l_g}{\mu_o A} + \frac{l_s}{2\mu_o \mu_r A} \qquad \begin{array}{c} -\alpha_o \le \alpha \le \alpha_o \\ or \\ \pi - \alpha_o \le \alpha \le \pi + \alpha_o \end{array} \tag{6.4.1}$$

where

$$\alpha_o = \arcsin\left(\frac{2h}{l_r}\right) \tag{6.4.2}$$

Therefore, from equations 6.3.1, 6.3.2, 6.3.3, 6.3.4, 6.4.1, and 6.4.2, the reluctance of the main magnetic flux path can be found by the following equation:

$$R_{rel}(\alpha) = R_A - R_B \frac{1}{|\sin(\alpha_o)|} \qquad \begin{matrix} -\alpha_o \le \alpha \le \alpha_o \\ or \\ \pi - \alpha_o \le \alpha \le \pi + \alpha_o \end{matrix} \tag{6.5.1}$$

$$R_{rel}(\alpha) = R_A - R_B \frac{1}{|\sin(\alpha)|} \qquad \begin{matrix} -\pi + \alpha_o < \alpha < -\alpha_o \\ or \\ \alpha_o < \alpha < \pi - \alpha_o \end{matrix} \tag{6.5.2}$$

where

$$R_A = \frac{2(l_r + 2l_g)\mu_r + l_s}{2\mu_o \mu_r A} \tag{6.5.3}$$

$$R_B = \frac{2h}{\mu_o A}\left(1 - \frac{1}{\mu_r}\right) \tag{6.5.4}$$

From equations 6.5.1 and 6.5.2, the reluctances of the main magnetic flux paths on the d-axis and the q-axis are:

$$R_{rel\_d} = R_{rel}(\alpha = 0) = R_A - R_B \frac{1}{|\sin(\alpha_o)|} \tag{6.6.1}$$

$$R_{rel\_q} = R_{rel}\left(\alpha = \frac{\pi}{2}\right) = R_A - R_B \tag{6.6.2}$$

Solving equations 6.6.1 and 6.6.2, for R_A and R_B gives:

$$R_A = \frac{1}{2}\left[R_{rel\_d} + R_{rel\_q} + (R_{rel\_q} - R_{rel\_d})\left(\frac{1 + |\sin(\alpha_o)|}{1 - |\sin(\alpha_o)|}\right)\right] \tag{6.7.1}$$

$$R_B = (R_{rel\_q} - R_{rel\_d})\left(\frac{|\sin(\alpha_o)|}{1 - |\sin(\alpha_o)|}\right) \tag{6.7.2}$$

By definition, the total magnetic flux is given by:

$$\Phi(\theta, \alpha, i) = \frac{F(\theta, \alpha, i)}{R_{rel}(\alpha)} = \frac{\lambda(\theta, \alpha, i)}{N} \tag{6.8}$$

where N is the number of turns of the winding linking the flux. Normalizing $F(\theta,\alpha,i)$ with respect to the number of turns of the field winding gives:

$$i_m(t) = \frac{F(\theta, \alpha, i)}{N_f} = F_{normal}(\theta, \alpha, i) \tag{6.9}$$

Therefore, the combining equations 6.8 and 6.9 gives

$$R_{rel}(\alpha) = \frac{F_{normal}(\theta, \alpha, i)}{\lambda_{normal}(\theta, \alpha, i)} \tag{6.10.1}$$

where

$$\lambda_{normal}(\theta, \alpha, i) = \frac{\lambda(\theta, \alpha, i)}{N_a} \tag{6.10.2}$$

$\lambda_{normal}(\theta,\alpha,i)$ is the normalized flux linkages with respect to the number of turns of phase-a winding.

By definition, the normalized flux linkages can be found by the following equation:

$$\lambda_{normal}(\theta, \alpha, i) = \frac{F_{normal}(\theta, \alpha, i)}{R_{rel}(\alpha)} \tag{6.11}$$

Combining equations 6.5.1, 6.5.2, and 6.11 gives the following new expression for the normalized flux linkage in the range of α:

$$\lambda_{normal}(\theta, \alpha, i) = \frac{F_{normal}(\theta, \alpha, i)}{R_A - R_B\left(\frac{1}{|\sin(\alpha_o)|}\right)} \qquad \begin{matrix} -\alpha_o \le \alpha \le \alpha_o \\ or \\ \pi - \alpha_o \le \alpha \le \pi + \alpha_o \end{matrix} \tag{6.12.1}$$

$$\lambda_{normal}(\theta, \alpha, i) = \frac{F_{normal}(\theta, \alpha, i)}{R_A - R_B\left(\frac{1}{|\sin(\alpha)|}\right)} \qquad \begin{matrix} -\pi + \alpha_o < \alpha < -\alpha_o \\ or \\ \alpha_o < \alpha < \pi - \alpha_o \end{matrix} \tag{6.12.2}$$

Equations 6.12.1 and 6.12.2 are used to generate other magnetizing curves when the magnetizing curves on the d-axis and q-axis are known. Therefore, these equations can be called magnetizing curve generating functions. Figure 6.3 shows some magnetizing curves produced by these equations based on the saturation curves in Figure 6.1.

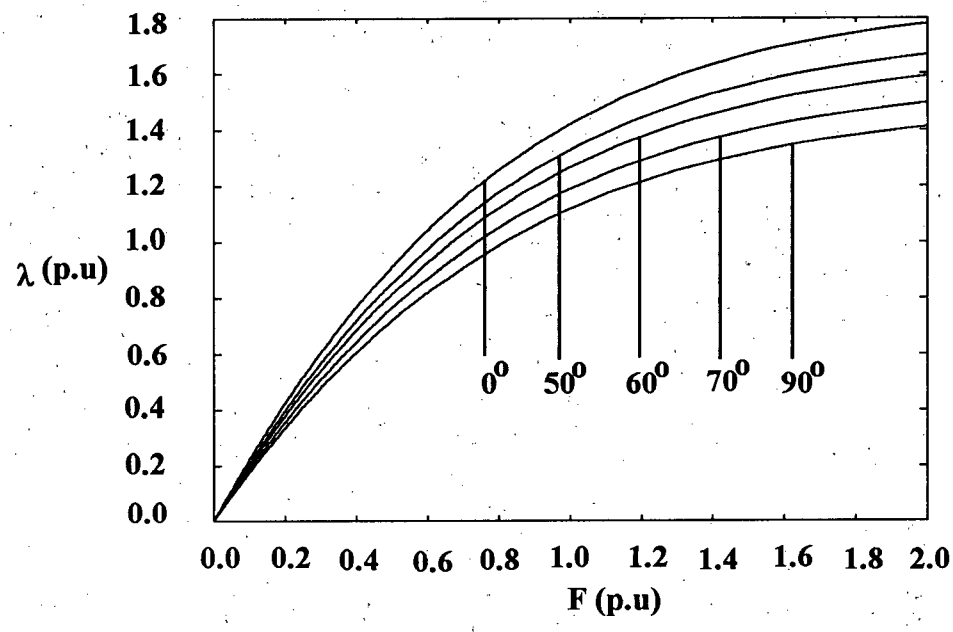

Figure 6.3 A Series of Magnetizing Curves Generated by the Magnetizing Curve Generating Functions

6.4 Inclusion of Magnetic Saturation Effects in the Generator Model

Once the magnetizing curve at a given angle α is known, the magnetic saturation effects can be incorporated in the model. The saturation curve is used to calculate the total flux linkages in the main magnetic path for different magnetizing currents (or magnetomotive forces). From the total flux linkages and the corresponding magnetizing currents (or magnetomotive forces), the changes of the inductances of the six magnetically coupled windings can be represented.

There are different approaches to calculating the flux linkages from the given saturation curve. Figure 6.4 shows two different methods[17,18,19].

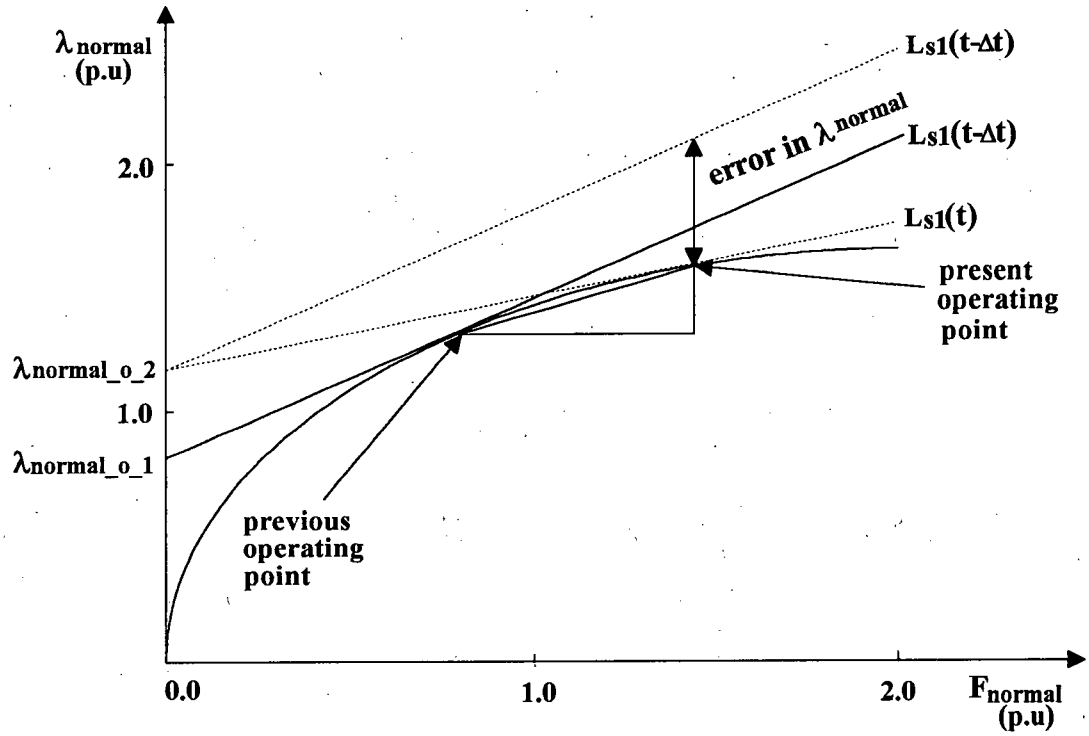

Figure 6.4 Two Different Methods to Calculate Flux Linkages

From Figure 6.4, $\lambda_{normal}(t)$ can be expressed exactly as follows:

$$\lambda_{normal}(t) = \lambda_{normal\_o\_1}(t) + L_{s1}(t)F_{normal}(t) \tag{6.13.1}$$

where $L_{s1}(t)$ is the slope of the line tangent to the magnetizing curve at the operating point.

However, using $L_{s1}(t-\Delta t)$ instead of $L_{s1}(t)$ results in a much different value of the normalized flux linkage:

$$\lambda_{normal}(t) = \lambda_{normal\_o\_2}(t) + L_{s1}(t-\Delta t)F_{normal}(t) \tag{6.13.2}$$

Equation 6.13.2 is represented by the dotted line in Figure 6.4 which gives a too different value of $\lambda_{normal}(t)$ from its true value.

The other method to calculate $\lambda_{normal}(t)$ is also indicated in Figure 6.4. In this approach, the normalized flux linkage is calculated from:

$$\lambda_{normal}(t) = \lambda_{normal}(t - \Delta t) + \Delta\lambda_{normal} \tag{6.14.1}$$

where

$$\Delta\lambda_{normal} = L_{s2}(t)[F_{normal}(t) - F_{normal}(t - \Delta t)] \tag{6.14.2}$$

$$L_{s2}(t) = \frac{\lambda_{normal}(t) - \lambda_{normal}(t - \Delta t)}{F_{normal}(t) - F_{normal}(t - \Delta t)} \tag{6.14.3}$$

$L_{s2}(t)$ is the slope of the line crossing the previous and the present operating points on the magnetizing curve and it also represents the total mutual inductance.

When there are no magnetic saturation effects, the total flux linkages are given by:

$$\lambda_{normal\_u}(t) = LF_{normal}(t) \tag{6.15}$$

where L is the slope of the air gap line.

Combining equations 6.14.1 and 6.15 gives:

$$\lambda_{normal}(t) = \lambda_{normal}(t - \Delta t) - \frac{L_{s2}(t)}{L}\lambda_{normal\_u}(t - \Delta t) + \frac{L_{s2}(t)}{L}\lambda_{normal\_u}(t) \tag{6.16}$$

The second presented method is preferred in the generator model because it calculates the flux linkages more accurately than the first presented method if the time step is small. After $L_{s2}(t)$ is determined, the flux linkages can be calculated, and consequently the induced voltages are calculated as follows:

$$[v_{induced}(t)] = \frac{d}{dt}[\lambda(t - \Delta t)] + \frac{d}{dt}[a(t)[L(t)]([i_m(t)] - i_m(t - \Delta t))] \tag{6.17.1}$$

where

$$a(t) = \frac{L_{s2}}{L} \tag{6.17.2}$$

$$[i_m(t)] = \frac{F(\theta, \alpha, i)}{N_f} = F_{normal}(t) = F_{normal}(\theta, \alpha, i) \tag{6.17.3}$$

To include the magnetic saturation effects in the synchronous machine, equation 3.8.1 should be corrected as follows:

$$[v(t)] = -[R][i(t)]$$
$$-\frac{d}{dt}[[\lambda(t-\Delta t)] + a(t)[L(t)]([i_m(t)] - [i_m(t-\Delta t)])] - [v_{rel}(t)] \qquad (6.18)$$

To verify the modelling of magnetic saturation effects in the proposed generator model, the magnetizing curves on the d-axis and the q-axis in Figure 6.1 are used to perform the simulation of a three-phase short-circuit at the machine terminals of a typical generator. The machine characteristic quantities are given in Table 6.1[20]. The generator is initially operated in steady state, then a three-phase short-circuit at the machine terminals occurs at t = 50 ms. Figures 6.5 and 6.6 show the terminal voltage and armature current of phase-a winding when saturation is included and excluded.

machine data		
Sr = 200.0 MVA	Xd = 1.70000000e00 pu	Xq = 1.64000000e00 pu
Vr = 13800.0 V	X'd = 2.3832400e-01 pu	X'q = 1.64000000e00 pu
ifo = 935.016 A	X"d = 1.846900e-01 pu	X"q = 1.851510e-01 pu
phase = 3	T'do = 6.194876e00 sec	T'qo = 0.000000e00 sec
poles = 2	T"do = 2.87160e-02 sec	T"qo = 7.49600e-02 sec
f = 60.0 Hz		
Ra = 1.0960000e-03 pu		
Xo = 1.40000000e00 pu		
Xl = 1.5000000e-01 pu		
single mass		
Jm = 7.632733e03 kg.m^2		
Dm = 0.0e00 Nm./(rad/s)		
Rexc = 0.000000e00 pu		

Table 6.1 The Data of a Typical Three-Phase Synchronous Generator

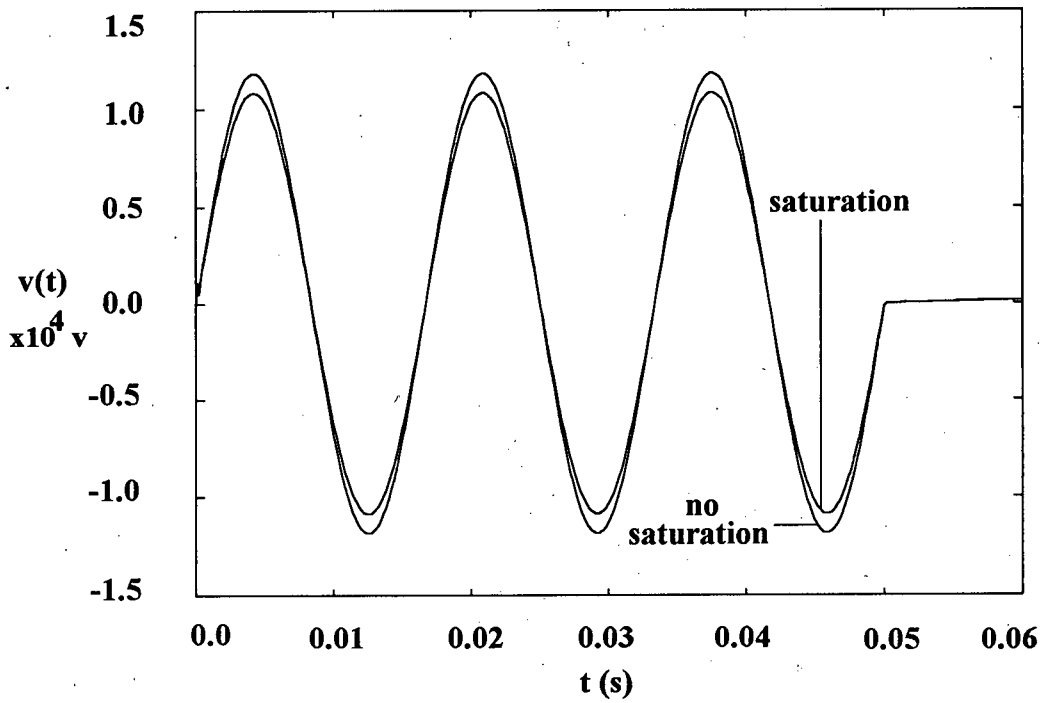

Figure 6.5 Terminal Voltage of Phase-a Winding with and without Saturation Effects when a Three-Phase Short-Circuit Occurs a t = 50 ms

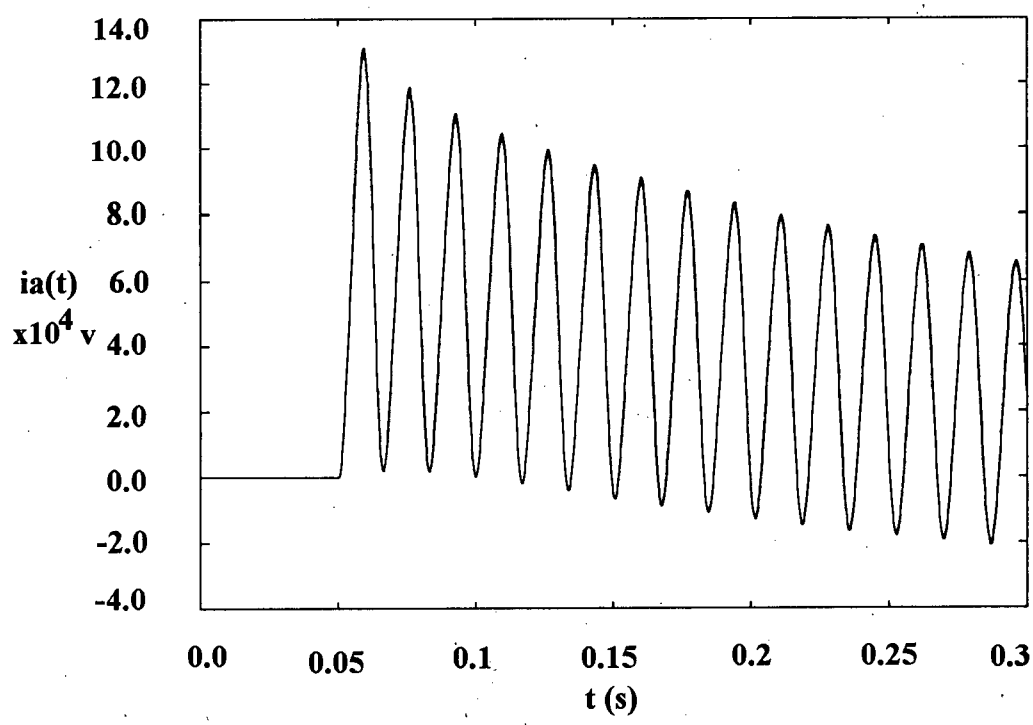

Figure 6.6 Current of Phase-a Winding with and without Saturation Effects when a Three-Phase Short-Circuit Occurs a t = 50 ms

Figure 6.5 shows that the induced terminal voltage of phase-a winding without considering saturation effects is higher than when saturation is included. From Figure 6.5 it can be been that the machine has been designed to operate in the saturated region in steady state. Figure 6.6 shows that for a three-phase short-circuit the current of phase-a winding obtained with the non-linear generator model is lower than that obtained with the linear model when the short-circuit just occurs. As time increases, the difference between the currents given by the two models becomes smaller and finally the currents are equal to each other.

Since the resistance of an armature winding is small compared to the synchronous reactance, the armature current lags the excitation voltage by almost 90°. Thus the stator's magnetomotive force almost opposes the field magnetomotive force. However, when the three-phase short-circuit first occurs, the armature currents are very large and the stator's magnetomotive force is larger than the field's. As a result, the combined magnetomotive force is still large and magnetic saturation takes place. As time elapses, the large oscillations in the armature currents are damped out and the stator's magnetomotive force becomes smaller. Consequently, the combined magnetomotive force becomes very small and no magnetic saturation occurs in the generator[21,22].

One practical implication of these results is that circuit breakers used to clear the fault have to initially sustain a smaller current than the value calculated without considering saturation and can, therefore, be more economically designed.

Chapter Seven

COMPARISON OF THE NEW MODEL WITH THE EMTP

7.1 Introduction

The proposed model of a three-phase synchronous generator without magnetic saturation is developed directly in the stator reference frame (abc co-ordinates). To verify the model, its performance can be compared with that of available generator models. In this chapter, the proposed abc model of a three-phase synchronous generator is compared with the dqo model in the EMTP. In addition, A case of a three-phase short-circuit at the machine terminals is simulated.

7.2 Evaluation of the Proposed abc Linear Generator Model

Since the proposed linear generator model directly represents a three-phase synchronous machine in the stator reference frame(abc co-ordinates), the inductances of the magnetically coupled windings depend on the rotor position. In the algorithm development, the values of these inductances need to be recalculated at each time step of the solution. The rotor position is needed to be predicted; however, this prediction introduces very small error due to the several orders of magnitude difference between the mechanical and electrical time constants in the machine.

A major advantage of developing the machine equations directly in the stator reference frame is that these equations can be solved simultaneously with the rest of the power system network. Thus the network is solved in abc co-ordinates and most of the problems of predictions or iterations that exist when the machine equations are solved in dqo reference frame are eliminated. This issue is particularly important in the context of on-line or real-

time simulators where the simulators are just turned on and expected to run continuously without losing numerical synchronization with the rest of the network. Working on abc co-ordinates also greatly simplifies the problem of representing the varying reluctance of the magnetic path between the rotor's d and q axis, as well as the different possible levels of saturation of these paths. A result of taking into account the difference in reluctance of the different magnetic paths is the inclusion of the "reluctance voltage" terms that do not appear in the dqo formulation in the machine equations. These reluctance voltage terms do not exist during steady state operation because the resultant magnetomotive force is fixed with respect to the rotor axis, but it exists under transient conditions.

7.3 Generator Model in the EMTP

The model of a three-phase synchronous generator in the EMTP is based on a discrete-time model in the rotor reference frame (dqo co-ordinates). The machine quantities are transformed between stator and rotor reference frames. Modelling a generator in the rotor reference frame eliminates the dependence of the winding inductances on the rotor position. That is, the inductances of the magnetically coupled coils that constitute the machine are time invariant in the rotor reference frame and there is no need to recalculate their values at each time step of the solution. The transformation of the machine quantities between the rotor and stator reference frames requires the use of Park's co-ordinate transformation. As already indicated, a main disadvantage of this approach is that the machine equivalent circuit (in dqo co-ordinates) cannot be solved simultaneously with the rest of the power system network (in abc co-ordinates). Prediction schemes are needed for the rotor position, current $i_d(t)$, current $i_q(t)$, speed voltage $u_d(t)$, and speed voltage $u_q(t)$.

7.4 Test of a Three-Phase Short-Circuit at the Machine Terminals

In order to assess the validity of the new generator machine model compared to the model in the EMTP, a three-phase short-circuit at the terminals of a three-phase synchronous generator was simulated. The machine description is given in Table 6.1. The generator is initially running in steady state and at time t = 5 ms, a three-phase short-circuit occurs at the machine terminals. Figures 7.1, 7.2, and 7.3 show the currents in the armature windings. The currents of the field structure windings are shown in Figures 7.4, 7.5, and 7.6. Finally, the torque on the shaft of the rotor and the rotor's speed are shown in Figures 7.7 and 7.8.

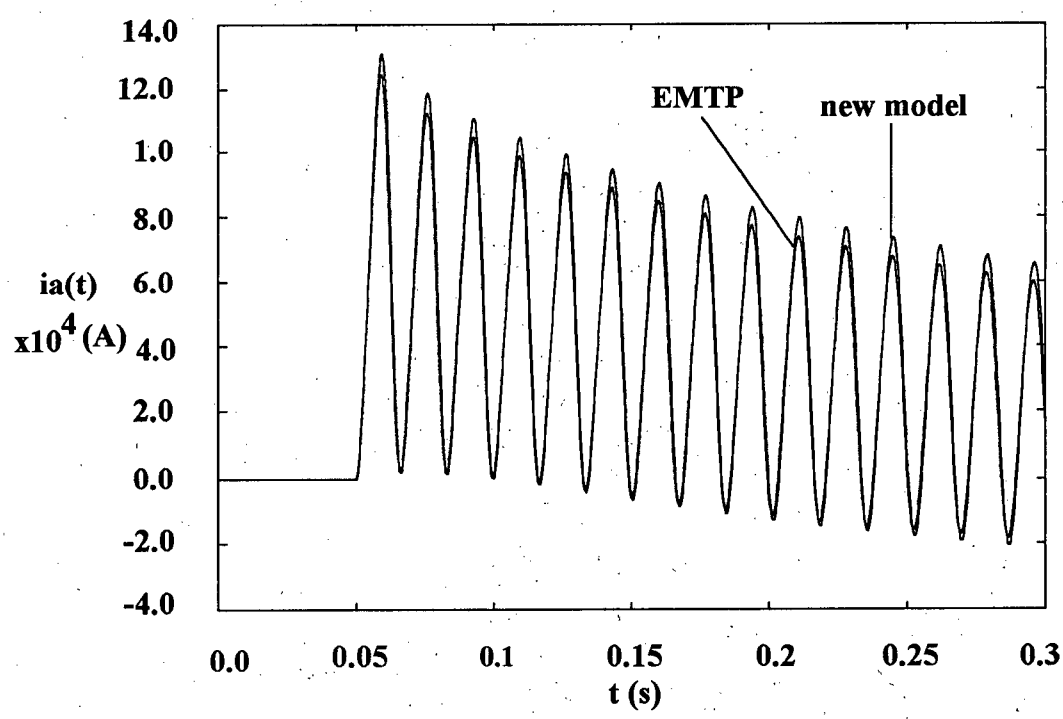

Figure 7.1 Current of Phase-a Winding Obtained with the New Model and the EMTP Model

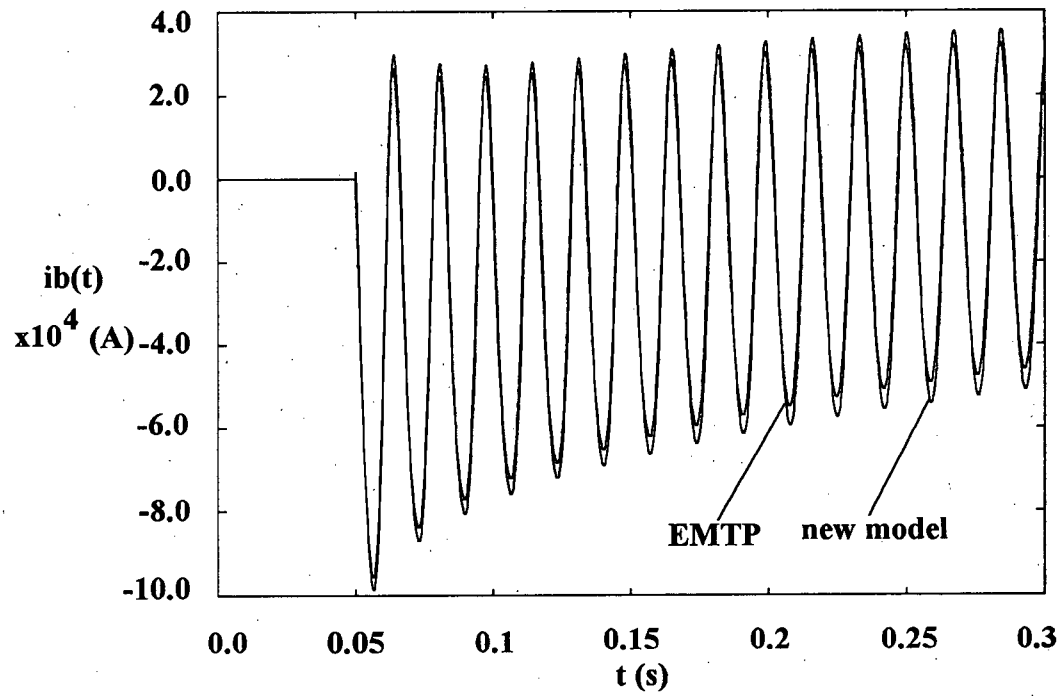

Figure 7.2 Current of Phase-b Winding Obtained with the New Model and the EMTP Model

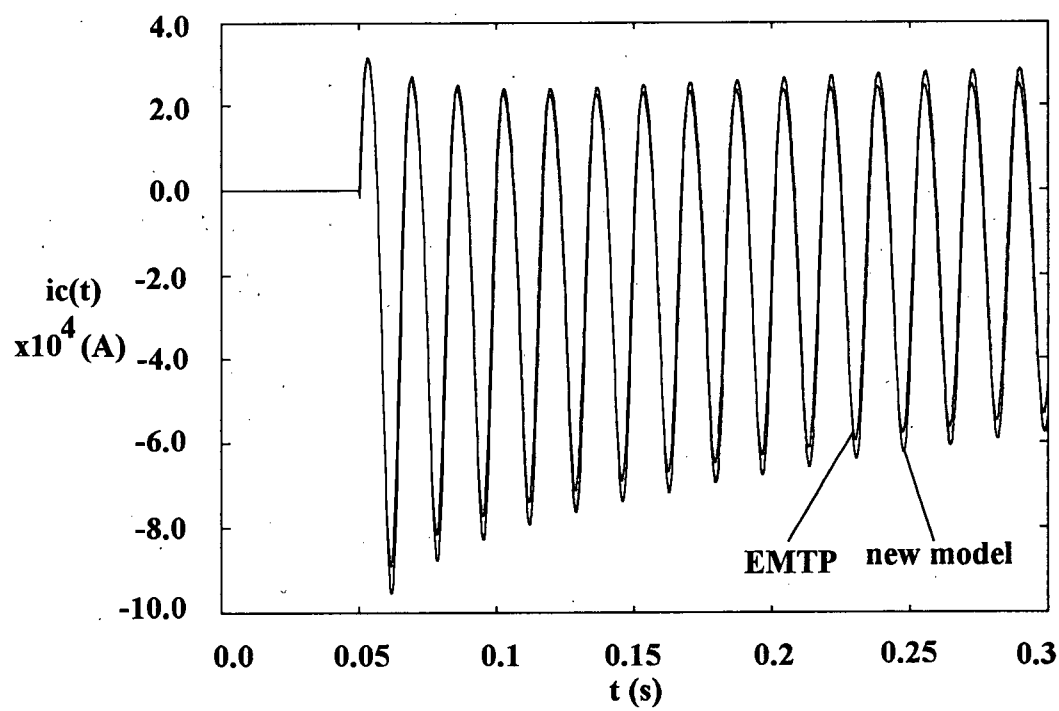

Figure 7.3 Current of Phase-c Winding Obtained with the New Model and the EMTP Model

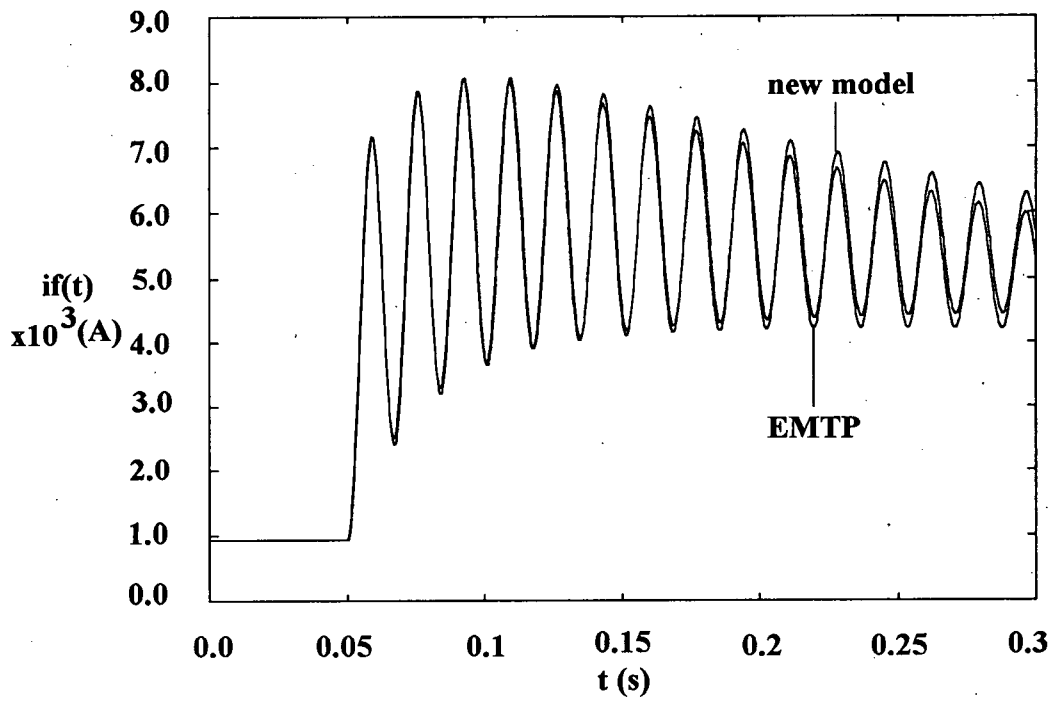

Figure 7.4 Field Current Obtained with the New Model and the EMTP Model

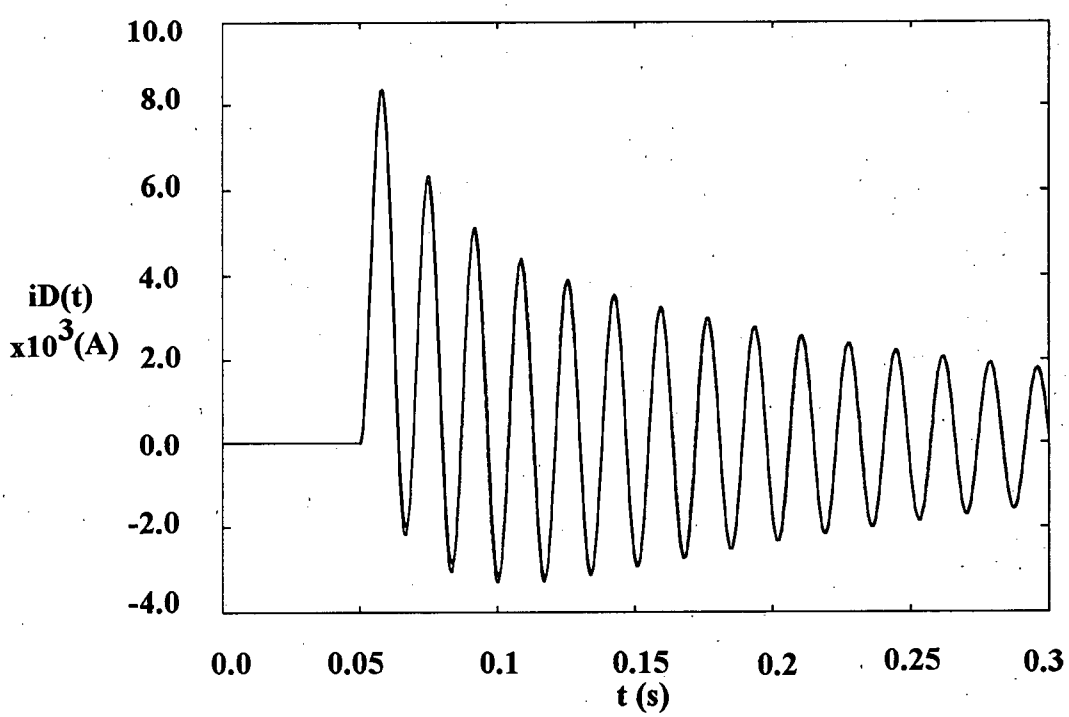

Figure 7.5 D-damper Current Obtained with the New Model and the EMTP Model

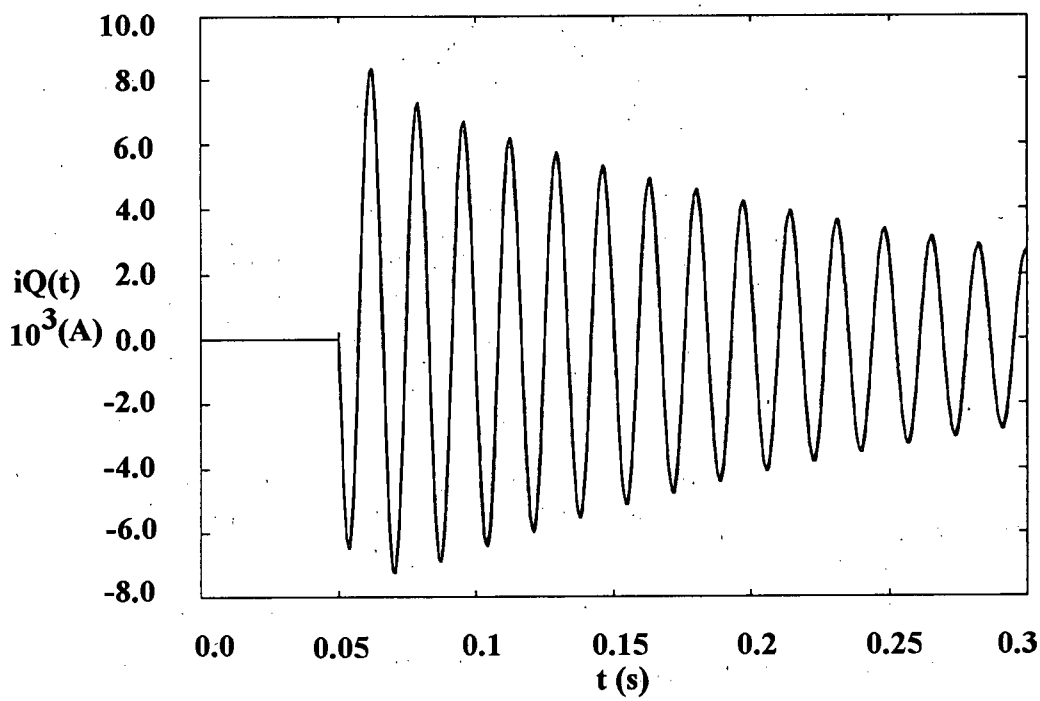

Figure 7.6 Q-damper Current Obtained with the New Model and the EMTP Model

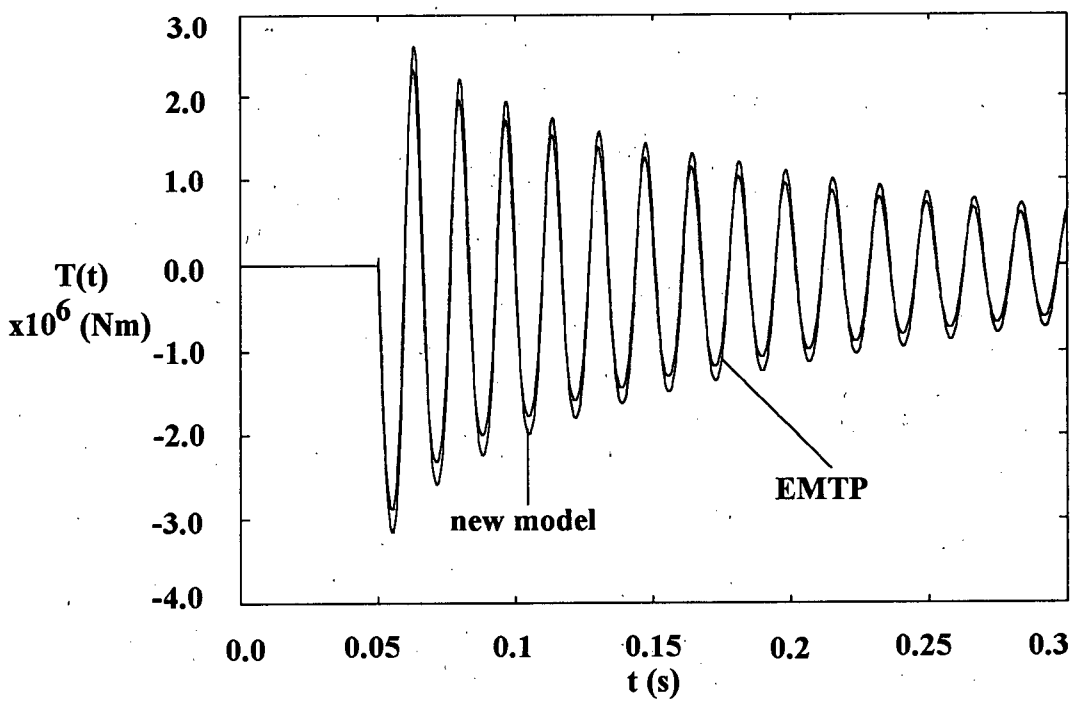

Figure 7.7 Torque on the Generator Shaft Obtained with the New Model and the EMTP Model

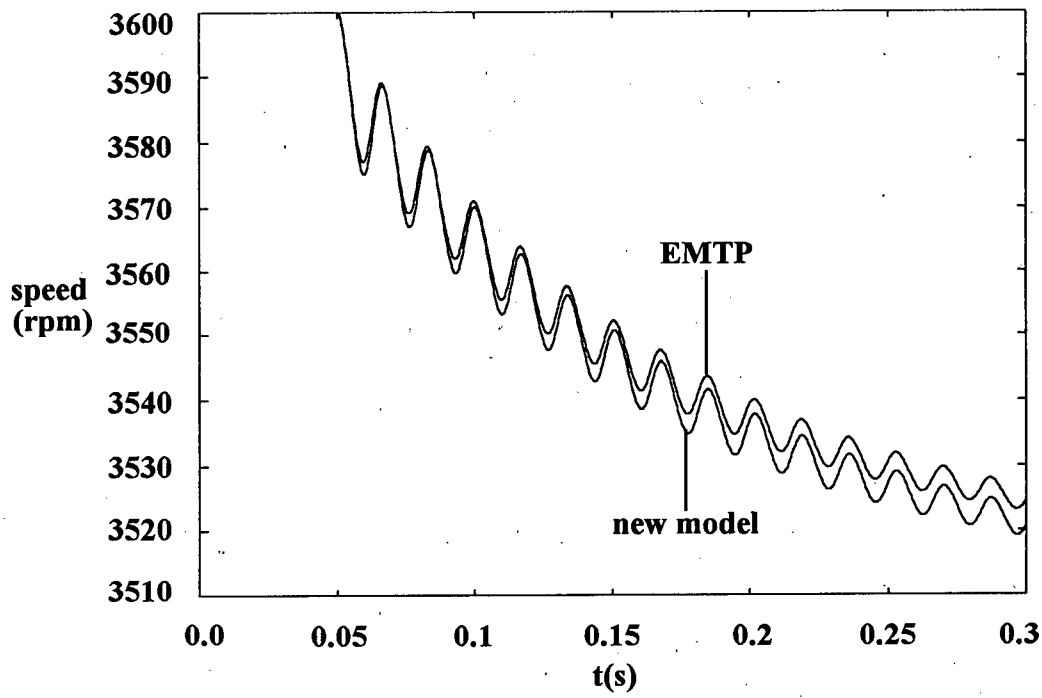

Figure 7.8 Rotor's Speed Obtained with the New Model and the EMTP Model

The currents in the armature windings obtained with the new model are slightly higher than those obtained with the EMTP model. The field current obtained with the new model is also higher than the current obtained with the EMTP model. The damper currents obtained with the two models, however, are very close to each other. The torques obtained with the now model is also slightly higher than the torque obtained with the EMTP model. However, the rotor speed obtained with the new model is lower than that obtained with the EMTP. The differences obtained are mainly due to the reluctance voltage correction in the new model. Figures 7.9, 7.10, and 7.11 show the field current, the current in phase-a winding, and the torque on the shaft obtained with the new model without the reluctance voltage correction and with the EMTP model. The results in this case agree with each other well.

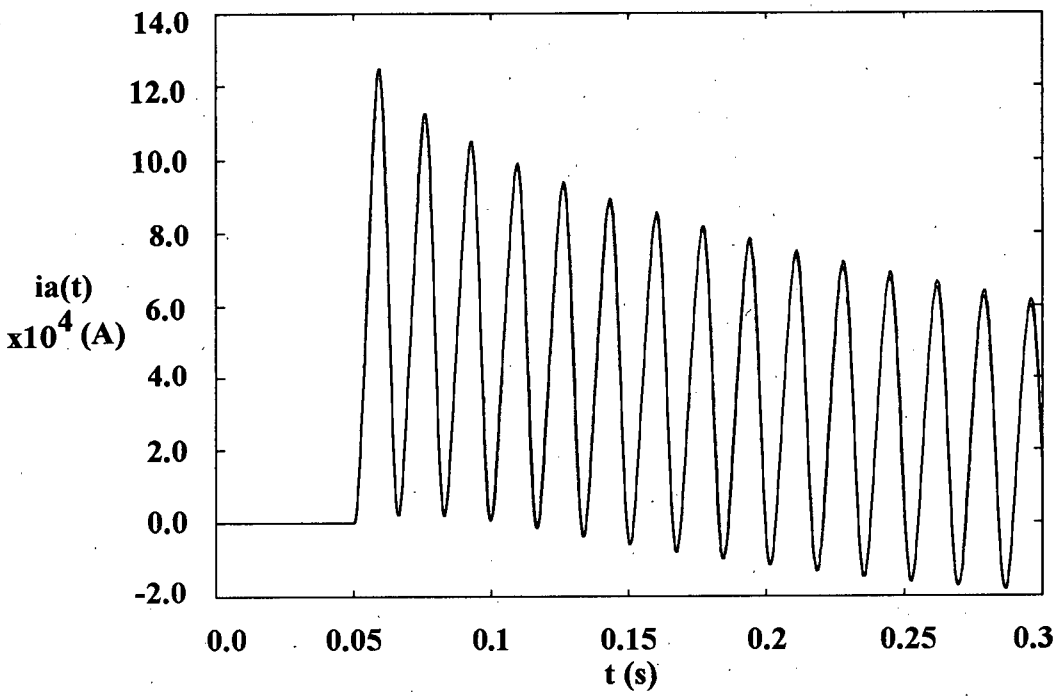

Figure 7.9 Current of Phase-a Winding Obtained with the New Model without Reluctance Voltage Correction Scheme and with the EMTP Model

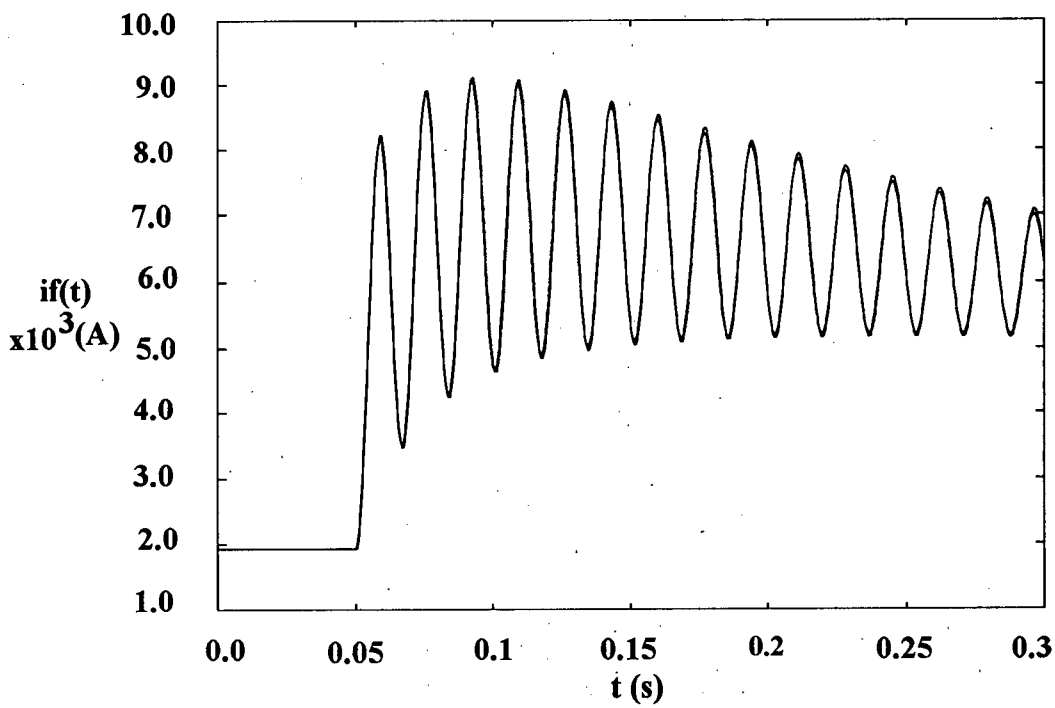

Figure 7.10 Field Current Obtained with the New Model without Reluctance Correction Scheme and with the EMTP Model

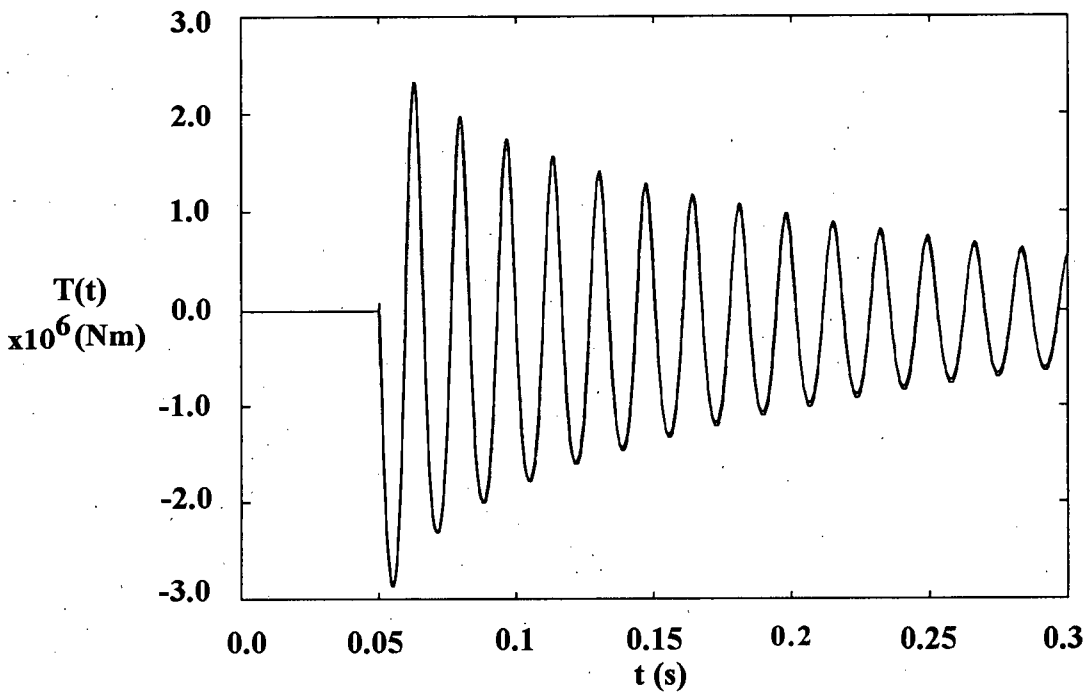

Figure 7.11 Torque Obtained with the New Model without Reluctance Voltage Correction Scheme and with the EMTP Model

These results indicate that the inclusion of the reluctance correction voltages in the generator model is important in modelling a salient pole three-phase synchronous machine. The new model directly establishes the discrete-time equations from the differential equations of the machine in the stator reference frame. While the EMTP model formulates the discrete-time equations from the machine differential equations in the rotor reference frame with the help of Park's co-ordinate transformation. Consequently, the new model has an advantage over the EMTP model in representing certain phenomena closely related to the machine's actual physical characteristics, such as saliency and saturation.

Chapter Eight

CONCLUSIONS

Three-phase synchronous generators are the main power sources in electric power systems. Since the performance of these machines greatly influence the operation of the networks, their accurate modelling is an important task. In this thesis a three-phase synchronous generator model has been built directly in the stator abc reference frame. It is a simpler generator model which does not need Park's co-ordinate transformation as conventional rotor-based dqo models.

In the model development, the differential equations of the machine's electrical and mechanical parts were first obtained separately. These equations were then put together by the rotor position and the electromagnetic torques exerted on the rotor's shaft by both the generator and the exciter machine. To take the variation of the main magnetic flux path in the generator into account, the differential equations of the machine's electrical part were corrected to include the reluctance voltages. These additional voltages were obtained from magnetizing curves. The machine's differential equations were discretized with the trapezoidal rule of integration, resulting in a discrete-time linear generator model. Based on the available magnetizing curves, magnetic saturation effects at any angle α were included in the generator model, thus resulting in a more accurate non-linear generator model. In order to obtain the necessary machine parameters needed in simulations, Canay's data conversion scheme was applied[23]. The model was coded into a computer program using the high level language of Ada95. A comparison between the performances of the new generator model and that in the EMTP was conducted to verify the validity of the new model. A three-phase short-circuit at the machine terminals was simulated with the new model and the EMTP model. The results obtained agreed with each other well when the reluctance

voltage terms were not included in the model. Again, The non-linear generator model produced conceptually consistent results of the behavior of a synchronous generator during a three-phase short-circuit.

REFERENCES

[1] Marti, J. R. and Lin, Jiming, "Suppression of Numerical Oscillations in the EMTP", IEEE, Trans, Vol. 4, No. 2, May 1989, pp.739-747.

[2] Lin, Jiming and Marti, J. R., "Implementation of the CDA Procedure in the EMTP", IEEE, Trans, Vol. 4, No. 2, May 1990, pp.394-402.

[3] Kundur, P., *Power System Stability And Control*, McGraw-Hill, Inc., New York, 1994.

[4] Adkins, B. and Harley, R. G., *The General Theory of Alternating Current Machines*, John Wiley & Sons, Inc., New York, 1975.

[5] Davis, H. F. and Snider, A. D., *Introduction to Vector Analysis*, Allyn and Bacon, Inc., Boston, 1979.

[6] Dommel, H. W., *EMTP Theory Book*, Microtran Power System Analysis, Corporation, Vancouver, 1992.

[7] Fowles, G. R., *Analytical Mechanics*, CBS College Publishing, New York, 1986.

[8] Streeter, V. L. and Wylie, E. B., *Fluid Mechanics*, McGraw-Hill, Inc., New York, 1985.

[9] Bergen, A. R., *Power System Analysis*, Prentice-Hall, Inc., New Jersey, 1986.

[10] Dommel

[11] Dommel

[12] Sarma, M. S., *Synchronous Machines: Theory, Stability, and Excitation System*, Gordon And Breach Science Publishers, New York, 1979.

[13] Lyon, W. V., *Transient Analysis of Alternating Current Machinery*, John Wiley & Sons, Inc., New York, 1954.

[14] Sarma

[15] Shields, P. C., *Elementary Linear Algebra*, Worth Publishers, Inc., New York, 1973.

[16] Dommel

[17] Abdel-Halim, M. A. and Manning C. D., "Modelling Saturation of Laminated Salient Pole Synchronous Machines", IEE Proc, Vol. 134, No. 4, July 1987, pp.215-223.

[18] Brandwajn, V., "Representation of Magnetic Saturation in the Synchronous Machine in an Electromagnetic Transient Program", IEEE Trans, Vol. Pas-99, No. 5, Sept/Oct, 1980, pp.1996-2002.

[19] Brown, J. E. and Kovacs, K. P. and Vas, P., "A Method of Including Effects of Main Flux Path Saturation In The Generalized Equations of A.C Machines", IEEE Trans, Vol. 102, No. 1, January 1983, pp.96-103.

[20] EMTP Development Co-ordination Group, EMTP WorkBook III, Electric Power Research Institute, Vol. 3, July 1989, pp.7.1-7.6.

[21] Sen, P. C., *Principle of Electric Machines and Power Electronics*, John Wiley & Sons., New York, 1989.

[22] Slemon, G. R. and Straughen, A., *Electric Machines*, Ontario, Addison-Wesley Publishing Company, 1981.

[23] Canay, I. M., "Determination of Model Parameters of Synchronous Machines", Proc. EE, Vol. 130, pt. B, March 1983, pp.86-94.

[24] Dommel

APPENDIX A

Flowchart Of The Computer Program For The New Generator Model

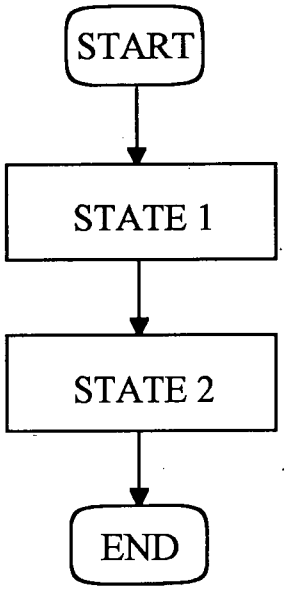

(a) Main Blocks of the Flowchart

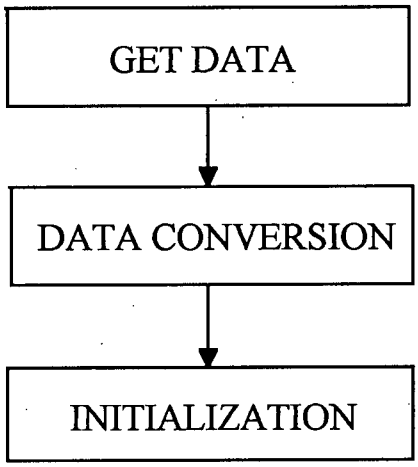

(b) Flowchart of State 1

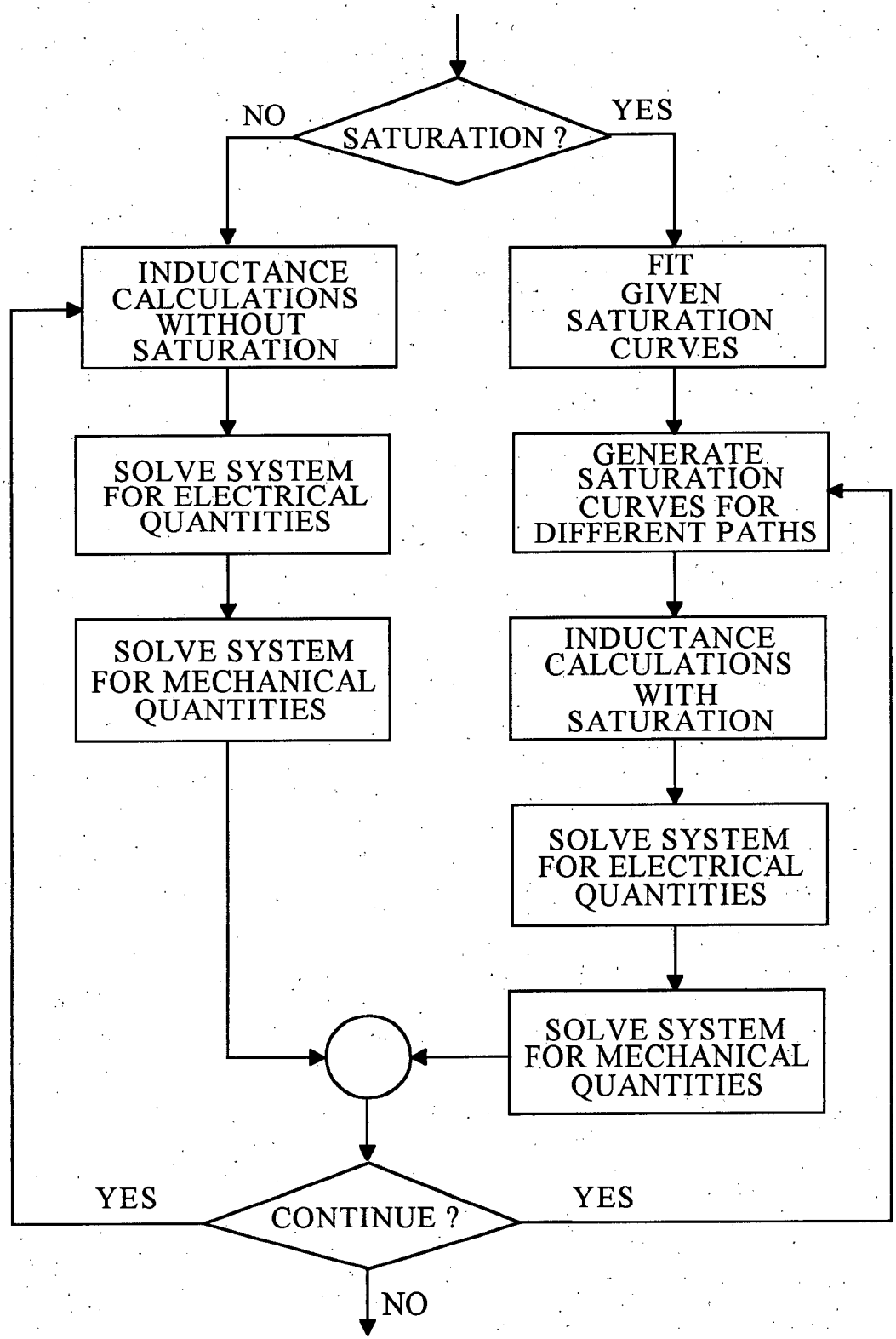

(c) Flowchart of State 2

APPENDIX B

EMTP Input File For The Three-Phase Short-Circuit Test

```
*                                   Case identification card
THREE-PHASE SHORT-CIRCUIT AT THE TERMINALS OF A THREE-PHASE
SYNCHRONOUS GENERATOR
*                                   Time Card
200.0E-6        2.0   1
*                                   Lumped RLC branch
LOADA           1.0E12
LOADB           1.0E12
LOADC           1.0E12
BUS3A           1.0E-5
BUS3B           1.0E-5
BUSEC           1.0E-5
$ = = =  End of level 1: Linear and nonlinear elements  = = = = = = = = = = = =
*
*                                   Time-controlled switch
   GENA     LOADA        -1.0     9999.0
   GENB     LOADB        -1.0     9999.0
   GENC     LOADC        -1.0     9999.0
   LOADA    BUS3A       5.0E-2    9999.0                          1.0E-3
   LOADB    BUS3B       5.0E-2    9999.0                          1.0E-3
   LOADC    BUS3C       5.0E-2    9999.0                          1.0E-3
$ = = =  End of level 2: Switches and piecewise linear elements  = = = = = = = = =
*
*                                   S.M. Node names for armature windings (Card 1)
50  GENA        60.0                11267.65     -90.0
*
*                                   S.M. Node names for armature windings (Card 2)
   GENB      2.0E2          1.38E1
*
*                                   S.M. Node names for armature windings (Card 3)
   GENC
*
*                                   S.M. Impedances and time constants (Card 4)
   1.096E-3    1.5E-1    1.7     1.64    2.38324E-1    1.64    1.8469E-1   1.85151
*
*                                   S.M. Impedances and time constants ( Card 5)
  6.194876    0.0    2.8716E-2    7.496E-2          1.4    9.35016E2
```

```
*
*  . . . . . .   S.M. output for electrical variables (Card 6)
11001110100
*
*  . . . . . .   S.M. Design parameters (Card 7)
   2     1     1     1
*
*  . . . . . .   S.M. Mass data (Card 8, 9, ect.)
                 1.0          0.007632733E6                    1 1
$> > > End of Synchronous Machine data mark < <
$ = = =  End of level 3: Sources  = = = = = = = = = = = = = = = = = = = = = = =
*
*  . . . . . .   voltage-output nodes
     GENA    GENB    GENC
$ = = = End of level 4: User-defined voltage output = = = = = = = = = = = = =
$ = = = Level 5: End of data case = = = = = = = = = = = = = = = = = = = = = = =
```

APPENDIX C

Data Conversion

This Appendix shows the data conversion procedure in EMTP Theory Book which was applied in the new generator model[24].

C.1 Given Machine Characteristic Quantities

According to IEEE or IEC standards, the available characteristic quantities of a generator are:

R_a(armature winding resistance),

X_l(armature winding leakage reactance),

X_o(zero sequence reactance),

X_d(synchronous reactance in d-axis),

X_q(synchronous reactance in q-axis),

X_d'(transient reactance in d-axis),

X_q'(transient reactance in q-axis),

X_d''(subtransient reactance in d-axis),

X_q''(subtransient reactance in q-axis),

T_d'(transient short-circuit time constant in d-axis),

T_q'(transient short-circuit time constant in q-axis),

T_d''(subtransient short-circuit time constant in d-axis),

T_q''(subtransient short-circuit time constant in q-axis).

However, sometimes the open-circuit time constants are given instead of short-circuit time constants:

T_{do}'(transient open-circuit time constant in d-axis),

T_{qo}'(transient open-circuit time constant in q-axis),

T_{do}''(subtransient open-circuit time constant in d-axis),

T_{qo}''(subtransient open-circuit time constant in q-axis).

C.2 Parameters in the Modified Rotor Reference Frame

If one set of the time constants is available, the other can be obtained by the following equations when neglecting R_a:

$$T'_{do} + T''_{do} = \frac{X_d}{X'_d} T'_d + \left(1 - \frac{X_d}{X'_d} + \frac{X_d}{X''_d}\right) T''_d \tag{C.1}$$

$$T'_{do} T''_{do} = T'_d T''_d \frac{X_d}{X''_d} \tag{C.2}$$

$$T'_{qo} + T''_{qo} = \frac{X_q}{X'_q} T'_q + (1 - \frac{X_q}{X'_q} + \frac{X_q}{X''_q}) T''_q \tag{C.3}$$

$$T'_{qo} T''_{qo} = T'_q T''_q \frac{X_q}{X''_q} \tag{C.4}$$

In the dqo reference frame, the flux linkages in both the d-axis and the q-axis are given by the following equations:

$$\begin{bmatrix} \lambda_d(t) \\ \lambda_f(t) \\ \lambda_D(t) \end{bmatrix} = \begin{bmatrix} L_d & M_{df} & M_{dD} \\ M_{df} & L_{ff} & M_{fD} \\ M_{dD} & M_{fD} & L_{DD} \end{bmatrix} \begin{bmatrix} i_d(t) \\ i_f(t) \\ i_D(t) \end{bmatrix} \tag{C.5}$$

$$\begin{bmatrix} \lambda_q(t) \\ \lambda_Q(t) \end{bmatrix} = \begin{bmatrix} L_q & M_{qQ} \\ M_{qQ} & L_{QQ} \end{bmatrix} \begin{bmatrix} i_q(t) \\ i_Q(t) \end{bmatrix} \tag{C.6}$$

where

$\lambda_d(t)$ and $\lambda_q(t)$ are flux linkages linking the d-winding and q-winding, respectively.

$i_d(t)$ and $i_q(t)$ are the currents passing through the d-winding and the q-winding, respectively.

L_d and L_q are the self inductances of the d-winding and the q-winding, respectively.

M_{df} is the mutual inductance between the d-winding and the field winding.

M_{dD} is the mutual inductance between the d-winding and the D-damper winding.

M_{fD} is the mutual inductance between the field winding and the D-damper winding.

M_{qQ} is the mutual inductance between the q-winding and the Q-damper winding.

In order to simplify the data conversion, the number of turns of the D-damper winding is chosen such that

$$M_{dD} = M_{df} \tag{C.7}$$

Traditionally, the field structure quantities are represented in the modified field structure as follows:

$$\lambda_{fm}(t) = \sqrt{\frac{3}{2}}\, k\lambda_f(t) \tag{C.8}$$

$$\lambda_{Dm}(t) = \sqrt{\frac{3}{2}}\, k\lambda_D(t) \tag{C.9}$$

$$\lambda_{Qm}(t) = \sqrt{\frac{3}{2}}\, k\lambda_Q(t) \tag{C.10}$$

$$i_{fm}(t) = \frac{1}{k}\sqrt{\frac{2}{3}}\, i_f(t) \tag{C.11}$$

$$i_{Dm}(t) = \frac{1}{k}\sqrt{\frac{2}{3}}\, i_D(t) \tag{C.12}$$

$$i_{Qm}(t) = \frac{1}{k}\sqrt{\frac{2}{3}}\, i_Q(t) \tag{C.13}$$

$$k = \frac{M_f}{M_{fD}} \tag{C.14}$$

Hence, in the modified field structure equations C5 and C6 become:

$$\begin{bmatrix} \lambda_d(t) \\ \lambda_{fm}(t) \\ \lambda_{Dm}(t) \end{bmatrix} = \begin{bmatrix} L_d & M_{md} & M_{md} \\ M_{md} & L_{ffm} & M_{md} \\ M_{md} & M_{md} & L_{DDm} \end{bmatrix} \begin{bmatrix} i_d(t) \\ i_{fm}(t) \\ i_{Dm}(t) \end{bmatrix} \tag{C.15}$$

$$\begin{bmatrix} \lambda_q(t) \\ \lambda_{Qm}(t) \end{bmatrix} = \begin{bmatrix} L_q & M_{mq} \\ M_{mq} & L_{QQm} \end{bmatrix} \begin{bmatrix} i_q(t) \\ i_{Qm}(t) \end{bmatrix} \tag{C.16}$$

where

M_{md} and M_{mq} are the mutual inductances on the d-axis and the q-axis in the modified field structure, respectively.

L_{ffm}, L_{DDm}, and L_{QQm} are the self inductances of the field winding, the D-damper winding, and the Q-damper winding in the modified field structure, respectively.

If k is known, the mutual inductance on the d-axis is given by:

$$L_c = L_d - \tfrac{3}{2}kM_f \tag{C.17}$$

$$M_{md} = L_d - L_c \tag{C.18}$$

However, if k is not given, then M_{md} becomes:

$$M_{md} = L_d - L_l \tag{C.19}$$

On the q-axis, the common mutual inductance is simply given by:

$$M_{mq} = L_q - L_l \tag{C.20}$$

Let R_{fm}, R_{Dm}, and R_{Qm} be the resistances of the field winding, the D-damper winding, and the Q-damper winding in the modified field structure, respectively. When k is not known, the voltage-current relationships of the windings in the modified dqo reference frame are:

$$\begin{bmatrix} v_d(t) \\ v_f(t) \\ 0 \end{bmatrix} = -\begin{bmatrix} R_a & 0 & 0 \\ 0 & R_{fm} & 0 \\ 0 & 0 & R_{Dm} \end{bmatrix} \begin{bmatrix} i_d(t) \\ i_{fm}(t) \\ i_{Dm}(t) \end{bmatrix} - \begin{bmatrix} L_d & M_{md} & M_{md} \\ M_{md} & L_{ffm} & M_{md} \\ M_{md} & M_{md} & L_{DDm} \end{bmatrix} \begin{bmatrix} \frac{di_d(t)}{dt} \\ \frac{di_{fm}(t)}{dt} \\ \frac{di_{Dm}(t)}{dt} \end{bmatrix} + \begin{bmatrix} -v'_d(t) \\ 0 \\ 0 \end{bmatrix} \tag{C.21}$$

$$\begin{bmatrix} v_q(t) \\ 0 \end{bmatrix} = -\begin{bmatrix} R_a & 0 \\ 0 & R_{Qm} \end{bmatrix} \begin{bmatrix} i_q(t) \\ i_{Qm}(t) \end{bmatrix} - \begin{bmatrix} L_q & M_{mq} \\ M_{mq} & L_{QQm} \end{bmatrix} \begin{bmatrix} \frac{di_q(t)}{dt} \\ \frac{di_Q(t)}{dt} \end{bmatrix} + \begin{bmatrix} -v'_q(t) \\ 0 \end{bmatrix} \tag{C.22}$$

Once M_{md} is known, the two time constants of the "f-branch" and the "D-branch" can be found. These time constants are given as follows:

$$T_1 = \frac{L_f}{R_f} \tag{C.23}$$

$$T_2 = \frac{L_D}{R_D} \tag{C.24}$$

where

$$L_f = L_{ff} - M_{md} \tag{C.25}$$

$$L_D = L_{DD} - M_{md} \tag{C.26}$$

The parallel inductance of M_{md}, L_f, and L_D is given by the following equation:

$$L_{parallelMfD} = L_d \frac{T'_d T''_d}{T'_{do} T''_{do}} - (L_d - M_{md}) \tag{C.27}$$

Once $L_{parallelMfD}$ is available, T_1 and T_2 can be calculated as follows:

$$T_1 + T_2 = (T'_{do} + T''_{do})\left(\frac{M_{md} - L_d}{M_{md}}\right) + (T'_d + T''_d)\frac{L_d}{M_{md}} \tag{C.28}$$

$$T_1 T_2 = T'_{do} T''_{do} \frac{L_{parallelMfD}}{M_{md}} \tag{C.29}$$

The parallel inductance of M_{md} and L_f is found by the following relationship:

$$L_{parallelMf} = \frac{M_{md}(T_1 - T_2)}{T'_{do} + T''_{do} - \left(1 + \frac{M_{md}}{L_{parallelMfD}}\right) T_2} \tag{C.30}$$

When $L_{parallelMfD}$ and $L_{parallelMf}$ are known, L_f and L_D are obtained by:

$$L_f = \frac{L_{parallelMf} M_{md}}{M_{md} - L_{parallelMf}} \tag{C.31}$$

$$L_D = \frac{L_{parallelMfD} - L_{parallelMf}}{L_{parallelMf} - L_{parallelMfD}} \tag{C.32}$$

Finally, the resistances and inductances in the modified field structure in the d-axis are:

$$R_{fm} = \frac{L_f}{T_1} \tag{C.33}$$

$$R_{Dm} = \frac{L_D}{T_2} \tag{C.34}$$

$$L_{ffm} = L_f + M_{md} \tag{C.35}$$

$$L_{DDm} = L_D + M_{md} \tag{C.36}$$

The inductance and the resistance of the Q-damper winding are obtained by the following equations:

$$\frac{1}{L_q''} - \frac{1}{L_q'} = -\frac{1}{L_q}\left[\frac{\omega T_q''\left(\omega T_q'' - \omega T_{qo}''\right)}{1+\left(\omega T_q''\right)^2}\right] \tag{C.37}$$

$$T_q'' = \frac{L_{QQm}}{R_{Qm}} \tag{C.38}$$

$$T_{qo}'' = \frac{L_{QQm} - \frac{M_{mq}^2}{L_q}}{R_{Qm}} \tag{C.39}$$

C.3 Conversion of dqo Quantities to the Stator Reference Frame

The machine parameters in the modified dqo reference frame are converted back to the unmodified field structure by the following equations:

$$L_{ff} = \frac{2}{3}\frac{L_{ffm}}{k^2} \tag{C.40}$$

$$L_{DD} = \frac{2}{3}\frac{L_{DDm}}{k^2} \tag{C.41}$$

$$L_{QQ} = \frac{2}{3}\frac{L_{QQm}}{k^2} \tag{C.42}$$

$$R_f = \frac{2}{3}\frac{R_{fm}}{k^2} \tag{C.43}$$

$$R_D = \frac{2}{3}\frac{R_{Dm}}{k^2} \tag{C.44}$$

$$R_Q = \frac{2}{3}\frac{R_{Qm}}{k^2} \tag{C.45}$$

Finally, the inductances in the dqo reference frame are converted back to the stator abc reference frame by the following equations:

$$M_f = \sqrt{\frac{2}{3}} M_{df} \tag{C.46}$$

$$M_D = \sqrt{\frac{2}{3}} M_{dD} \tag{C.47}$$

$$M_Q = \sqrt{\frac{2}{3}} M_{qQ} \tag{C.48}$$

$$L_s = \frac{L_d + L_q + L_o}{3} \tag{C.49}$$

$$L_m = \frac{L_d - L_q}{3} \tag{C.50}$$

$$M_s = \frac{2L_o - L_d - L_q}{6} \tag{C.51}$$